Meccanica manuscript No.
(will be inserted by the editor)

Homogenized modeling for vascularized poroelastic materials

Raimondo Penta · José Merodio

Received: date / Accepted: date

Abstract A new mathematical model for the macroscopic behavior of a material composed of a poroelastic solid embedding a Newtonian fluid network phase (also referred to as *vascularized poroelastic material*), with fluid transport between them, is derived via asymptotic homogenization. The typical distance between the vessels/channels (*microscale*) is much smaller than the average size of a whole domain (*macroscale*). The homogeneous and isotropic Biot's equation (in the quasi-static case and in absence of volume forces) for the poroelastic phase and the Stokes' problem for the fluid network are coupled through a fluid-structure interaction problem which accounts for fluid transport between the two phases; the latter is driven by the pressure difference between the two compartments. The averaging process results in a new system of partial differential equations (PDEs) that formally reads as a *double poroelastic*, globally mass conserving, model, together with a new constitutive relationship for the whole material which encodes the role of both pore and the fluid network pressures. The mathematical model describes the mutual interplay among fluid filling the pores, flow in the network, transport between compartments, and linear elastic deformation of the (potentially compressible) elastic matrix comprising the poroelastic phase. Assuming periodicity at the microscale level, the model is computationally feasible, as it holds on the macroscale only (where the microstructure is smoothed out), and encodes geometrical information on the microvessels in its coefficients, which are to be computed solving classical periodic cell problems. Recently developed *double porosity models* are recovered when deformations of the elastic matrix are neglected. The new model is relevant to a wide range of applications, such as fluid in porous, fractured rocks, blood transport in vascularized, deformable tumors, and interactions across different hierarchical levels of porosity in the bone.

Keywords Poroelasticity · Fluid-structure interaction · Fluid transport · Double porosity · Multiscale expansion · Asymptotic homogenization · Hierarchical materials · Vascularized tumors

R. Penta
Departamento de Mecanica de los Medios Continuos y T. Estructuras, E.T.S. de caminos, canales y puertos, Universidad Politecnica de Madrid, Calle Profesor Aranguren S/N, 28040, Madrid, Spain.
Tel.: +34/913366659
Fax: +34/913366702
E-mail: raimondo.penta@upm.es

J. Merodio
Departamento de Mecanica de los Medios Continuos y T. Estructuras, E.T.S. de caminos, canales y puertos, Universidad Politecnica de Madrid, Calle Profesor Aranguren S/N, 28040, Madrid, Spain.
Tel.: +34/913365391
Fax: +34/913366702
E-mail: jose.merodio@upm.es

1 Introduction

The interplay between a deformable, porous solid and a fluid network phase (i.e. made of vessels, channels, or connected cavities) concerns a large variety of real-world physical scenarios, such as groundwater aquifers and petroleum reservoirs, hard biological tissues, and organs/cell aggregates. These systems are often *multiscale*, and possibly hierarchical in nature. The spatial scale characterizing the fluid flow in the pores is much smaller than the typical length scale of the network. Such a scale is, in turn, much smaller than the average, macroscopic size of the hierarchical level of the system

under investigation. The latter can be a portion of tissue, rock, organ, etc. that contains a high number of vessels (or channels, cavities), such that the difference between two of them cannot be resolved on such a scale.

Relevant examples include fluid flowing in relatively large fractures and *vugs*, interacting with porous and deformable rocks [2], fluid transport across the membrane of tubular cavities interacting with the bone mineralized matrix [14] (which is made of collagen, mineral and water [44]), as well as blood extravasating from the vascular walls to the healthy and tumor tissue [23, 24]. Most of these physical systems can be viewed, from a modeling perspective, as *poroelastic* media interacting with a viscous fluid phase. Here we focus on these media and we define them as *vascularized poroelastic materials*.

The theory of poroelasticity ([6, 7, 8, 9, 10]) has been extensively adopted for continuum modeling of solids such as rocks [43], the mineralized collagen matrix in the bone [14], and healthy and malignant cell aggregates [11]. The equations of poroelasticity can be derived "averaging" the interactions between fluid filling the pores and the deformable comprising matrix, resulting in a system of partial differential equations (PDEs) that can effectively represent the physics of the system even though the pore geometry itself is smoothed out. The upscaling process can be carried out via several approaches, such as effective medium theory, volume averaging, mixture theory, and asymptotic homogenization (also known as two-scale homogenization or multiscale homogenization), see, e.g. the comprehensive review [5]. Average fields techniques, such as effective medium theory, can provide an estimate of the coefficients, and related bounds, for a limited number of particular cases, exploiting the semi-analytical results due to Eshelby [18], where the different phases are represented as elliptical inclusions. The mixture theory and volume averaging approaches allow for generality in the constitutive behavior of the constituents, and can provide some characterizations of the coefficients on the basis of physical considerations. The *asymptotic homogenization* technique exploits the length scale separation that exists in the system to derive the effective governing equations of (linearized) poroelasticity retaining the information on the porescale, which are encoded in the coefficients of the model (see [13]). The latter are prescribed in terms of the solution of differential problems to be solved on the porescale geometry. Therefore, this approach is powerful as it provides the appropriate structure of the governing PDEs and precise pore scale prescriptions for the coefficients. However, it is necessary to assume periodicity of the pore scale structure to actually solve the pore scale problems in practice, and this approach cannot be trivially extended to nonlinear constitutive equations for the fluid and the elastic phases.

The physical system that we consider in this work can be studied, from a mechanical viewpoint, as a *fluid-structure interaction* problem. The structure and the fluid are represented by an elastic, porous medium (that can be modeled via the theory of poroelasticity) and a viscous fluid (that is typically considered Newtonian), respectively. There exist several examples in the context of poroelasticity, see, e.g. [42] and [17], where the coupling between the poroelastic and viscous compartments is carried out analytically (for slightly compressible phases and negligible in inertia) and numerically (for intrinsically incompressible phases, and accounting for inertia in the context of hemodynamic applications), respectively.

The three dimensional solution of such a problem would be almost impossible from a practical (computational) viewpoint, due to the large number of microvessels' interactions to be resolved. Furthermore, experimental measurements are usually performed at an averaged, tissue level (see, e.g., [22, 23, 24] where examples of measurements of tumor blood flow determinants are reported). These arguments motivate the development of a multiscale approach which can provide an effective model capable to describe the macroscopic and constitutive behavior of the system on a *macroscale*; such a scale should be representative of the whole system and much bigger than the intervessel (channels) distance. At the same time, it is of crucial importance to retain information on the geometrical complexity of the fluid network phase.

In this work, we embrace the asymptotic homogenization technique to derive a novel mathematical model for the macroscale representation of vascularized poroelastic materials.

We first setup a fluid structure interaction problem between a linearized poroelastic material and a low-Reynolds number fluid, governed by the linear and isotropic Biot's equations and the Stokes' problem, respectively. We neglect inertia, body forces, and assume that both the fluid in the pores and in the network is incompressible, whereas compressibility of the solid phase is permitted. The two compartments are coupled via appropriate interface conditions that account for (a) *conservation of momentum* (via prescription of continuity of the global stresses), (b) *fluid mass conservation*, relating normal components of velocities to account for possible compressibility of the solid phase, (c) *slip over the porous surface*, prescribing the tangential component of the fluid network stress, which is assumed to be proportional to the tangent component

of fluid network velocity (relative to the solid velocity) [4], (d) *transport of fluid across the interface* between the two compartments, prescribing that the difference between the normal component of the fluid stresses is proportional to the normal component of the fluid network velocity (relative to the solid velocity). The latter condition is particularly important to address transport of fluid across the interface, as it represents the rigorous formalization of a phenomenological relationship (also known as Starling's law [41]) that relates the fluid flux across the vessels membrane to the difference between the poroelatic (interstitial) and vessels' pressure. This relationship is adapted from [34] to account for possible (linear elastic) deformations of the porous compartment, and ignoring contribution due to passive scalars (e.g. drugs), which are not considered in this work.

We define an asymptotic small parameter as the ratio between the *microscale*, which is the intervessels (channels) distance, and the *macroscale*, i.e. the average size of the whole vascularized poroelastic material. We perform an appropriate non-dimensionalization step to account for the asymptotic behavior of the various parameters arising in the formulation, following and adapting the physical considerations reported in [34] to the case of a deformable porous structure. We then introduce and apply the asymptotic homogenization technique (see, e.g., [1, 3, 20, 27, 31, 39]), representing the relevant field as power series in terms of the small asymptotic parameter in the light of the sharp length scale separation that exists in the system. We further assume periodicity to better compare the results to previously derived double porosity models and to provide coefficients' prescriptions that can be used for practical applications at a reduced computational cost.

We obtain a new macroscale system of PDEs in terms of the zero-th order pressures, velocities and elastic displacement. The mathematical model is formally of *double poroelastic* type, and effectively accounts for the fluid transport between the poroelastic and the fluid network compartments through source terms which are proportional to the difference in pressure. The mutual influence of time variations of the pressures due to deformations of the solid matrix comprising the poroelastic compartment appear explicitly. The model is globally mass conserving and the coefficients are to be computed solving standard periodic problems on a geometry which is representative of the microvessels.

The model reads as a significant generalization of the existing *double porosity* fluid transport model recently derived in the context of rigid, vascularized tumors in [41] and [34][1]), and solved via a semi-analytical approach in [33] for a tortuous microvasculature. The latter model is recovered as a particular case for a rigid solid compartment. The reminder of this work is organized as follows.

In Section 2 we setup the fluid-structure interaction problem between the poroelastic compartment and the fluid network. In Section 3 we perform a nondimensional analysis and enforce appropriate physical arguments to justify the asymptotic behavior of the model parameters. In Section 4 we introduce the asymptotic homogenization technique and formulate the two-scale setting of the problem. In Section 5 we apply the asymptotic homogenization technique to systematically derive the new model. In Section 6 we discuss the computational feasibility and the physical meaning of the model. The double porosity model [34, 41] is recovered as a particular case for rigid solid structures. In Section 7 we draw conclusions and highlight further perspectives.

2 Governing equations

We consider a set $\Omega \subset \mathbb{R}^3$, such that $\bar{\Omega} = \bar{\Omega}_p \cup \bar{\Omega}_n$, where Ω_p and Ω_n represent the poroelastic and fluid network compartment, respectively. We assume that the typical pore scale r is much smaller than the distance between two adjacent vessels/channels d. Thus, on the scale d, we account for an already smoothed out geometry of the porous structure (see Figure 1), and it is therefore appropriate to account for a poroelastic modeling of the solid porous compartment, rather than considering the interaction between two distinct fluid phases and the elastic matrix. A similar argument is exploited in [41] (page 1466, Section 2.1), where the interaction between a (rigid) tumor mass and its blood vessels' network is addressed assuming that the tumor can be modeled as a porous medium (satisfying Darcy's law). In that case, the authors assume that the typical pore scale (i.e. the inter-cell separation in the tumor) is much smaller than the intercapillary distance characterizing the network of blood vessels.

We assume that the intervessel distance d is, in turn, much smaller than the average size of the domain L, i.e., we define a small parameter ϵ satisfying

$$\epsilon = \frac{d}{L} \ll 1. \tag{1}$$

The difference between the scales characterizing the problem is highlighted in Figure 1.

[1] These two paper differ in some scaling assumptions concerning the drug transport analysis, but the double porosity fluid transport models, for a purely Newtonian blood vessels' rheology and for macroscopically uniform media, coincide, as actually demonstrated in [34].

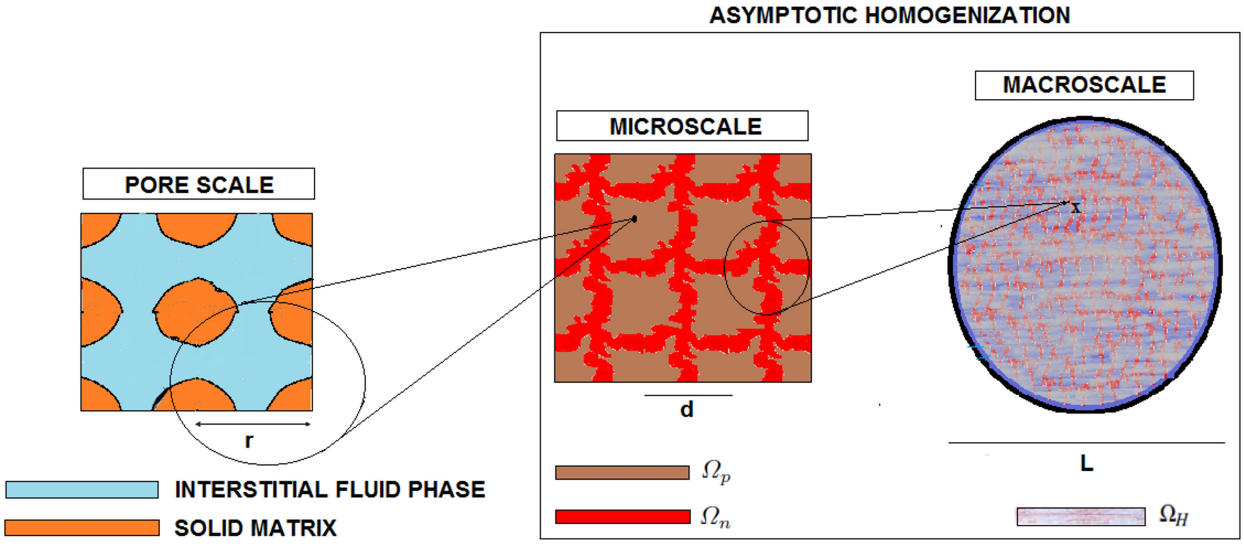

Fig. 1 A 2D schematic of the pore scale, microscale, and macroscale, which satisfy $r \ll d \ll L$. On the left, the typical pore scale r, which is much smaller than the intervessel distance d. On the right, the *asymptotic homogenization* block shows the difference between the microscale d, where the difference between the vessels and the porous solid can be clearly identified, and the typical macroscale L, which characterizes the homogenized domain Ω_H where the network geometry is smoothed out.

We first state the governing equations for the poroelastic and the fluid compartments, and then close the resulting system of partial differential equations (PDEs) via appropriate interface conditions on the interface $\Gamma = \partial\Omega_p \cap \partial\Omega_n$. Every variable is in general a function of space $\boldsymbol{x}$ and time t.

2.1 The poroelastic compartment

We assume that linear, isotropic, and homogeneous Biot's poroelasticity holds in the compartment Ω_p.

We consider a quasi-static regime (as done, for example in [29]), and neglect body forces for the sake of simplicity. The stress balance equation in the poroelastic compartment then reads

$$\nabla \cdot \mathsf{T_p} = 0 \ , \text{in } \Omega_p, \tag{2}$$

where the poroelastic stress tensor $\mathsf{T_p}$ is defined by

$$\mathsf{T_p} = \mathbb{C} : \nabla \boldsymbol{u} - \tilde{\alpha} p_p \mathsf{I}, \tag{3}$$

where $\boldsymbol{u}$ is the displacement of the porous matrix, p_p is the interstitial pressure of the fluid in the pores, $\tilde{\alpha}$ is the Biot coefficient, that depends on the porosity, geometry of the porous structure and the elastic constants of the elastic phase, and $\mathbb{C}$ is the stiffness tensor of the poroelastic medium. The operation " : " represents the standard double contraction, by components notation $\mathbb{C} : \nabla \boldsymbol{u}$ reads

$$C_{ijkl} \frac{\partial u_k}{\partial x_l}, \tag{4}$$

where $i, j, k, l = 1, 2, 3$ and summation over repeated indices is understood. The elasticity tensor $\mathbb{C}$ is equipped with the standard major and (left and right) minor symmetries (see, e.g. [19]), the latter implying

$$\mathbb{C} : \nabla \boldsymbol{u} = \mathbb{C} : \xi(\boldsymbol{u}), \tag{5}$$

where

$$\xi = \frac{\nabla \boldsymbol{u} + (\nabla \boldsymbol{u})^{\mathsf{T}}}{2} \tag{6}$$

is the strain tensor associated with the displacement $\boldsymbol{u}$. Assuming an isotropic constitutive relationship we have

$$\mathbb{C} : \xi(\boldsymbol{u}) = \lambda (\nabla \cdot \boldsymbol{u}) \mathsf{I} + 2\mu_e \xi(\boldsymbol{u}). \tag{7}$$

Here, λ and μ_e denote the Lamé constants of the poroelastic material. In particular, λ is the so called *drained* Lamé constant (i.e. that of an equivalent elastic material with empty pores, that is, setting $p_p = 0$) and μ_e the shear modulus. Both constants are related to the elastic properties of the comprising matrix, but they differ, in general, from the latter, as they also depend on the interstitial porosity and geometry of the pore scale structure.

The pressure in the pores p_p and the interstitial (pore) fluid velocity $\boldsymbol{v}_p$ are related to each other via Darcy's law

$$\boldsymbol{w}_p = -\frac{k}{\mu} \nabla p_p, \tag{8}$$

where k is the permeability of the poroelastic medium, μ the fluid viscosity, and $\boldsymbol{w}_p$ denotes the relative interstitial velocity, i.e.

$$\boldsymbol{w}_p = \phi\,(\boldsymbol{v}_p - \dot{\boldsymbol{u}})\,, \tag{9}$$

where the $\dot{(\bullet)}$ operator denotes the time derivative and ϕ is the interstitial porosity, i.e. the ratio between the interstitial fluid volume and the volume of the whole poroelastic compartment. [2] The mass conservation relationship for the poroelastic compartment reads:

$$\dot{p}_p = -\tilde{\alpha} M \nabla \cdot \dot{\boldsymbol{u}} - M \nabla \cdot \boldsymbol{w}_p, \tag{10}$$

where M denotes the Biot modulus.

Remark 1 (On the relationship between pore pressure and fluid content)
Relationship (10) combines the balance of fluid content with the standard constitutive equation which relates the pore pressure to the change in fluid content and volume of an isotropic Biot's porous medium (see, e.g., [16, 32]). In our notation, such a constitutive relationship reads

$$p_p = -\tilde{\alpha} M \nabla \cdot \boldsymbol{u} + M \Xi, \tag{11}$$

where Ξ represents the fluid content. The latter can be in turn related to the fluid flux (which is here denoted by $\boldsymbol{w}_p$ and referred to as the relative interstitial velocity) via the standard continuity equation which holds in absence of external fluid sources (see, e.g., [16])

$$\dot{\Xi} + \nabla \cdot \boldsymbol{w}_p = 0. \tag{12}$$

Finally, differentiating relationship (11) with respect to time and then substituting the continuity equation (12) yields equation (10). □

The Biot modulus M can be viewed as the inverse of the variation of the fluid volume in response to a variation of pore pressure, for constant strain (that is, the lower M, the higher the variation of fluid volume in response to the pore pressure variations is). It is a poroelastic coefficient that depends on the pore scale geometry and porosity, on the properties of the comprising elastic matrix, and on the fluid bulk modulus [13]. The coefficient M is proportional to the fluid bulk modulus when the solid phase only is incompressible (see, e.g. [16]), whereas, when the fluid phase only is incompressible, M solely depends on the pore scale geometry, porosity, and properties of the comprising elastic matrix (see, e.g. [13] and the no-growth limit section of [35]). Whenever both the fluid and the solid phase are intrinsically incompressible, $M \to +\infty$. From equation (10), we can also deduce the physical meaning of the Biot coefficient $\tilde{\alpha}$, which can be interpreted as the ratio of increase (decrease) of interstitial fluid volume to solid volume changes. The upper bound $\tilde{\alpha} = 1$ is reached whenever both the solid and the interstitial fluid phase are intrinsically incompressible. In such a case, $M \to +\infty$ and the two volume variations exactly balance, so $\tilde{\alpha} = 1$ and relationship (10) reads

$$\nabla \cdot \boldsymbol{w}_p + \nabla \cdot \dot{\boldsymbol{u}} = 0, \tag{13}$$

or, if the interstitial porosity ϕ can be considered homogeneous

$$\phi \nabla \cdot \boldsymbol{v}_p + (1-\phi) \nabla \cdot \dot{\boldsymbol{u}} = 0. \tag{14}$$

Here, we allow for compressibility of the solid phase, i.e. $0 < \tilde{\alpha} \leq 1$. Concerning the interstitial fluid phase, since we are coupling it with the incompressible Newtonian fluid phase in the network, we then consider that also the fluid phase in the pores is intrinsically incompressible for the sake of consistency. However, a potential dependency of Biot's modulus M on the fluid bulk modulus would not appear in the derivation that follows in the next sections.

Remark 2 (On the assumption of isotropy) The assumption of isotropy can be easily relaxed and is enforced here solely (a) to clearly highlight the physical meaning of parameters (b) to reduce the number of input parameters that are eventually needed to solve the derived homogenized model presented in the next sections (c) to avoid complicating the notation, also considering that anisotropic values for poroelastic parameters are rarely provided by the experimental literature. However, whenever this is the case, or, alternatively, the latter are known directly from the pore scale structure, then the more general anisotropic setting should be considered. It is worth noting that we actually never explicitly enforce isotropy of $\mathbb{C}$ in the analysis that follow (although it is considered isotropic for the sake of consistency with the other parameters), and that the Biot modulus reads as a scalar also for anisotropic poroelastic media. Hence, from the technical point of view, the framework provided here can be readily generalized to anisotropy considering that the term $\tilde{\alpha} \nabla \cdot \dot{\boldsymbol{u}}$ reads as (following [13] in our notation)

$$(\phi \mathsf{I} - \mathsf{D}) : \nabla \dot{\boldsymbol{u}}, \tag{15}$$

[2] The vector field $\boldsymbol{w}_p$ that satisfies Darcy's law (8) actually represents the average relative fluid velocity in the porous medium and is also referred to as the discharge, flux, or filtration velocity. It is indeed related to the specific relative velocity $\boldsymbol{v}_p - \dot{\boldsymbol{u}}$ via the interstitial porosity ϕ. However, since we conveniently carry out our analysis in terms of $\boldsymbol{w}_p$ hereinafter, we simply refer to $\boldsymbol{w}_p$ as the *relative interstitial velocity*.

where D is a second rank tensor that depends on the elasticity tensor of the solid matrix and on the pore scale structure in terms of porosity and geometry. □

2.2 The fluid network

We consider an incompressible Newtonian fluid phase in the network Ω_n and neglect inertial effects and volume forces, such that the following Stokes' problem holds

$$\nabla \cdot \mathsf{T}_n = 0 \tag{16}$$

$$\nabla \cdot \boldsymbol{v}_n = 0, \tag{17}$$

where T_n denotes the fluid network stress tensor defined by

$$\mathsf{T}_n = -p_n \mathsf{I} + \mu \left(\nabla \boldsymbol{v}_n + (\nabla \boldsymbol{v}_n)^{\mathsf{T}} \right) \tag{18}$$

and $\boldsymbol{v}_n$, p_n are the fluid network velocity and pressure, respectively.

2.3 Interface coupling

We assume continuity of poroelastic and fluid network stresses (which is to be enforced as a consequence of global conservation of momentum), i.e.

$$\mathsf{T}_n \boldsymbol{n} = \mathsf{T}_p \boldsymbol{n} \text{ on } \Gamma, \tag{19}$$

where $\boldsymbol{n}$ is the unit outward vector normal to the fluid network surface. The normal component of the relative fluid velocity at the interface between the poroelastic compartment and the fluid network is related to that of the solid phase by the following relationship

$$\boldsymbol{v}_n \cdot \boldsymbol{n} = (\tilde{\alpha} \dot{\boldsymbol{u}} + \boldsymbol{w}_p) \cdot \boldsymbol{n} \text{ on } \Gamma, \tag{20}$$

or equivalently

$$(\boldsymbol{v}_n - \dot{\boldsymbol{u}}) \cdot \boldsymbol{n} = ((\tilde{\alpha} - 1)\dot{\boldsymbol{u}} + \boldsymbol{w}_p) \cdot \boldsymbol{n} \text{ on } \Gamma. \tag{21}$$

The condition (20) reads as the correct admissibility constraint on the interface Γ for normal fluid fluxes to ensure mass conservation when possible compressibility of the solid matrix is considered. Such a compatibility condition is enforced, for example, in the study [42], where the fluid-structure interaction between a Biot's poroelastic system and the Stokes' flow is analyzed.[3] Whenever the interstitial fluid and solid matrix phases of the poroelastic compartment are intrinsically incompressible, $\tilde{\alpha} = 1$, so that

$$(\boldsymbol{v}_n - \dot{\boldsymbol{u}}) \cdot \boldsymbol{n} = \boldsymbol{w}_p \cdot \boldsymbol{n} \text{ on } \Gamma, \tag{22}$$

[3] Our admissibility constraint (20) is equivalent to equation (2.a), page 7, [42], setting their $\beta = 0$ and considering that c_0, $\boldsymbol{v}^1$, $\boldsymbol{v}^2$, and $\boldsymbol{q}$ are denoted by $\tilde{\alpha}$, $\dot{\boldsymbol{u}}$, $\boldsymbol{u}_n$, $\boldsymbol{w}_p$ in our manuscript.

as shown for example in [17].

We now discuss the appropriate prescriptions for the normal and tangential component of the fluid network stress to account for fluid transport between the two compartments and fluid slip over a porous surface, respectively.

2.3.1 Fluid transport across the interface

We aim to describe fluid transport across the interface between the poroelastic and the fluid network compartment. We embrace the non-equilibrium thermodynamical approach derived by Kedem and Katchalsky [26] and adopted in [34], where the fluid flux Φ_n is related to the pressure drop across the interface between the two compartments. The original formulation also involves a contribution related to the jump of osmotic pressures due to possible solute, which is not considered here as we are not dealing with passive scalar transport (such as drugs) in this work. We therefore seek for an heuristic relationship (also called *Starling's law* as in [24, 41]) of the type

$$\Phi_n \propto S(p_n - p_p), \tag{23}$$

where S is the total surface of the vessels/channels forming the network. According to the considerations carried out in [34] (where the authors deal with fluid and drug extravasation across the tumor vessels' network), the physics encoded in the relationship of the type (23) should be formalized as an interface condition that relates the normal component of the fluid network velocity to the difference between the fluid network normal stress and the fluid pressure in the porous compartment. We therefore assume the following non-equilibrium interface condition, that describes fluid transport across the interface between the poroelastic matrix and the fluid network

$$(\boldsymbol{v}_n - \dot{\boldsymbol{u}}) \cdot \boldsymbol{n} = -L_p \left(\boldsymbol{n} \cdot (\mathsf{T}_n \boldsymbol{n}) + p_p \right), \tag{24}$$

where L_p quantifies the leakage of fluid from the vessels/channels and is also referred to as the hydraulic conductivity of the microvascular walls in the biophysical literature concerning solid tumors, as in [24].

Now we ensure that the total fluid flux (proportional to the pressure drop across the interface multiplied by the total vessels surface) stays finite whenever more and more vessels/channels are considered in a fixed portion of the domain (or, equivalently when considering the limit $\epsilon \to 0$, cf. (1)). According to [34] (Remark 2.3, page 9), this issue can be tackled considering that the parameter L_p (and, in general, any parameter describing transport across the interface) is typically measured considering the total fluid flux. Since the latter is in

turn proportional also to the total vessels surface, which scales with the number of vessels (i.e. $\propto 1/\epsilon$), it is assumed that the specific (per unit surface) flux scales as $O(\epsilon)$. We account for this asymptotic behavior of the fluid flux redefining

$$\epsilon L^* = L_p, \tag{25}$$

Substituting (25) in (24) and rearranging terms yields

$$\boldsymbol{n} \cdot (\mathsf{T}_n \boldsymbol{n}) + \frac{1}{\epsilon L^*}(\boldsymbol{v}_n - \dot{\boldsymbol{u}}) \cdot \boldsymbol{n} = -p_p, \tag{26}$$

which reads, in our notation, as the corresponding interface condition assumed in [34] for vascularized tumors, adapted considering that the solid matrix is moving and that no drug transport is taken into account here.

2.3.2 Slip over a porous surface

We account for the fluid slip over a porous surface assuming the Beavers-Joseph-Saffman conditions (see [4, 25, 38]), rearranged as done in [17] to relate the tangential components of the fluid network stress and relative velocity, i.e.

$$\boldsymbol{\tau}_\beta \cdot (\mathsf{T}_n \boldsymbol{n}) = -\frac{\alpha\mu}{\sqrt{k}}(\boldsymbol{v}_n - \dot{\boldsymbol{u}}) \cdot \boldsymbol{\tau}_\beta, \text{ on } \Gamma, \tag{27}$$

where $\beta = 1, 2$, α is the non-dimensional Beavers and Joseph parameter which depends on the properties of the porous interface, the $\boldsymbol{\tau}_\beta$ denote the unit vectors tangent to the interface and k is the permeability of the poroelastic compartment that appears in the Darcy equation (8).

3 The non-dimensional system of PDEs

Equations (2, 3), (8), (10) for the poroelastic compartment Ω_p, together with relationships (16, 18), (17) for the fluid network compartment Ω_n, and the interface conditions (19), (21), (26), (27) on Γ, represent a closed system of PDEs on the whole domain Ω in terms of the variables $\boldsymbol{u}$, $\boldsymbol{w}_p$, $\boldsymbol{v}_n$, p_p, p_n, provided that appropriate initial conditions and external boundary conditions on $\partial\Omega$ are prescribed, depending on the specific physical system at hand.

Now we non-dimensionalize variables as follows:

$$\begin{aligned}&\boldsymbol{x} = L\boldsymbol{x'},\ \boldsymbol{u} = L\boldsymbol{u'},\ \boldsymbol{v}_p = \frac{Cd^2}{\mu}\boldsymbol{v}'_p,\ p_p = CLp'_p,\\ &\mathbb{C} = CL\mathbb{C}',\ t = \frac{L\mu}{Cd^2}t',\ \boldsymbol{v}_n = \frac{Cd^2}{\mu}\boldsymbol{v}'_n,\ p_n = CLp'_n,\end{aligned} \tag{28}$$

where C is a reference pressure gradient. We then non-dimensionalize the poroelastic and fluid network stress tensors T_p and T_n, as well as the relative interstitial velocity $\boldsymbol{w}_p$, consistently with (28), i.e.

$$\mathsf{T}_n = CL\mathsf{T}'_n,\ \mathsf{T}_p = CL\mathsf{T}'_p,\ \boldsymbol{w}_p = \frac{Cd^2}{\mu}\boldsymbol{w}'_p. \tag{29}$$

Since $\nabla(\bullet) = \frac{1}{L}\nabla'(\bullet)$, neglecting the primes for the sake of simplicity of notation yields the following non-dimensional system of PDEs, for every $\boldsymbol{x} \in \Omega$ and for every $t \in (0, T)$, $T \in \mathbb{R}^+$

$$\nabla \cdot \mathsf{T}_\mathsf{p} = 0, \text{ in } \Omega_p \tag{30}$$

$$\mathsf{T}_\mathsf{p} = \mathbb{C} : \nabla\boldsymbol{u} - \tilde{\alpha}p_p\mathsf{I} \tag{31}$$

$$\boldsymbol{w}_p = -\bar{k}\nabla p_p, \text{ in } \Omega_p \tag{32}$$

$$\dot{p}_p = -\tilde{\alpha}\bar{M}\nabla \cdot \dot{\boldsymbol{u}} - \bar{M}\nabla \cdot \boldsymbol{w}_p \text{ in } \Omega_p \tag{33}$$

$$\nabla \cdot \mathsf{T}_n = 0, \text{ in } \Omega_n \tag{34}$$

$$\mathsf{T}_n = -p_n\mathsf{I} + \epsilon^2\left(\nabla\boldsymbol{v}_n + (\nabla\boldsymbol{v}_n)^\mathsf{T}\right) \tag{35}$$

$$\nabla \cdot \boldsymbol{v}_n = 0, \text{ in } \Omega_n, \tag{36}$$

supplemented by the following interface conditions

$$\mathsf{T}_n\boldsymbol{n} = \mathsf{T}_p\boldsymbol{n} \text{ on } \Gamma, \tag{37}$$

$$(\boldsymbol{v}_n - \dot{\boldsymbol{u}}) \cdot \boldsymbol{n} = ((\tilde{\alpha} - 1)\dot{\boldsymbol{u}} + \boldsymbol{w}_p) \cdot \boldsymbol{n} \text{ on } \Gamma, \tag{38}$$

$$\boldsymbol{\tau}_\beta \cdot (\mathsf{T}_n\boldsymbol{n}) = -\epsilon\frac{\alpha}{\sqrt{\bar{k}}}(\boldsymbol{v}_n - \dot{\boldsymbol{u}}) \cdot \boldsymbol{\tau}_\beta, \text{ on } \Gamma, \tag{39}$$

$$\boldsymbol{n} \cdot (\mathsf{T}_n\boldsymbol{n}) + \frac{1}{\epsilon\bar{L}_p}(\boldsymbol{v}_n - \dot{\boldsymbol{u}}) \cdot \boldsymbol{n} = -p_p \text{ on } \Gamma. \tag{40}$$

The newly introduced non-dimensional numbers read

$$\bar{k} = \frac{k}{d^2},\ \bar{L}_p = \frac{L^*L\mu}{d^2} = \frac{L_pL^2\mu}{d^3},\ \bar{M} = \frac{M}{CL}. \tag{41}$$

Here, $\bar{L}_p$, $\bar{k}$, and $\bar{M}$ are the non-dimensional interface hydraulic conductivity, porous compartment permeability, and Biot's modulus, respectively.

Remark 3 (The characteristic Stokes' velocity profile) We have scaled velocities with respect the Stokes'-type characteristic velocity profile

$$U = \frac{Cd^2}{\mu}. \tag{42}$$

The latter choice preserves the asymptotic behavior of the relative pore velocity $\boldsymbol{w}_p$ when the distance between the vessels/channels in the network decreases (i.e. when $\epsilon \to 0$), as done in [34] for the interstitial flow coupled to the blood vessels network. The same scaling is applied to the network velocity and to the solid velocity $\dot{\boldsymbol{u}}$ (as the time is non-dimensionalized with respect to the time scale dictated by U (cf. (28))), consistently with definition (9) and continuity condition (38). This choice formally leads to the typical ϵ^2 scaling which arises when upscaling Newtonian-type flow (cf. equation (35)), as also noted in [35]. □

Every non-dimensional number arising in the system (30-40) is considered fixed in the limit $\epsilon \to 0$ to account for the greatest possible number of physical phenomena in the analysis that follows, as done in [34]. The non-dimensional permeability $\bar{k}$ and $\bar{L}_p$ are formally analogous to their counterpart in the works [34, 41], where the effective governing equations for fluid transport in vascularized rigid tumors are derived and discussed.

4 Two-scale homogenization

We now apply the asymptotic homogenization technique (see, for example, [20, 21, 27, 31, 39, 40]) to derive a new set of macroscale governing equations for the system of PDEs (30-40) that describes vascularized poroelastic materials. In the light of the sharp length scale separation between the microscale and the macroscale, i.e.

$$\epsilon \ll 1 \tag{43}$$

we introduce a new spatial variable

$$\boldsymbol{y} = \frac{\boldsymbol{x}}{\epsilon} \tag{44}$$

to map microscopic variations of the fields. We decouple spatial variations, such that $\boldsymbol{x}$ and $\boldsymbol{y}$ are considered formally independent variables that account for macroscale and microscale spatial variations, respectively. We assume that the fields p_p, p_n, $\boldsymbol{w}_p$, $\boldsymbol{v}_n$, $\boldsymbol{u}$, T_p, T_n are functions of both $\boldsymbol{x}$ and $\boldsymbol{y}$. As a consequence, differential operators transform according to

$$\nabla \to \nabla_{\boldsymbol{x}} + \frac{1}{\epsilon}\nabla_{\boldsymbol{y}}. \tag{45}$$

We employ the following power series representation for every field (denoted collectively by $\tilde{f}$)

$$\tilde{f} \equiv \tilde{f}^{\epsilon}(\boldsymbol{x}, \boldsymbol{y}, t) = \sum_{l=0}^{\infty} \tilde{f}^{(l)}(\boldsymbol{x}, \boldsymbol{y}, t)\epsilon^l. \tag{46}$$

Each component $\tilde{f}^{(l)}$ is defined for every $\boldsymbol{x}$ belonging to the macroscale domain Ω_H, while $\boldsymbol{y}$ maps microscale variations in the appropriate subdomain where $\tilde{f}$ is defined. Finally, we account for appropriate regularity assumptions for the fields with respect to the newly introduced microscale variable $\boldsymbol{y}$. Although boundedness with respect to the local spatial variable $\boldsymbol{y}$ would be in principle sufficient to derive the new set of governing equations (see, e.g. the derivation of the Biot's poroelasticity carried out in [13]), we aim to provide suitable prescriptions for the coefficients of the macroscale model that can be practically computed on a reduced portion of the domain. Hence, following the commonly exploited approach in the multiscale asymptotics literature, we assume that every field is periodic with respect to the local variable $\boldsymbol{y}$.

Exploiting the representation (46) and the spatial scale decoupling (45), equations (30-40) read (after multiplying each of them by a suitable power of ϵ)

$$\nabla_{\boldsymbol{y}} \cdot \mathsf{T}_p^{\epsilon} + \epsilon \nabla_{\boldsymbol{x}} \cdot \mathsf{T}_p^{\epsilon} = 0 \text{ in } \Omega_p, \tag{47}$$

$$\epsilon \mathsf{T}_p^{\epsilon} = \mathbb{C}\nabla_{\boldsymbol{y}} \boldsymbol{u}^{\epsilon} + \epsilon \mathbb{C}\nabla_{\boldsymbol{x}} \boldsymbol{u}^{\epsilon} - \epsilon \tilde{\alpha} p_p^{\epsilon} \mathsf{I}, \text{ in } \Omega_p, \tag{48}$$

$$\epsilon \boldsymbol{w}_p^{\epsilon} = -\bar{k}\nabla_{\boldsymbol{y}} p_p^{\epsilon} - \epsilon \bar{k}\nabla_{\boldsymbol{x}} p_p^{\epsilon} \text{ in } \Omega_p, \tag{49}$$

$$\begin{aligned}\epsilon \dot{p}_p^{\epsilon} &= -\tilde{\alpha}\bar{M}\nabla_{\boldsymbol{y}} \cdot \dot{\boldsymbol{u}}^{\epsilon} - \bar{M}\nabla_{\boldsymbol{y}} \cdot \boldsymbol{w}_p^{\epsilon} \\ &- \epsilon\tilde{\alpha}\bar{M}\nabla_{\boldsymbol{x}} \cdot \dot{\boldsymbol{u}}^{\epsilon} - \epsilon\bar{M}\nabla_{\boldsymbol{x}} \cdot \boldsymbol{w}_p^{\epsilon} \text{ in } \Omega_p,\end{aligned} \tag{50}$$

$$\nabla_{\boldsymbol{y}} \cdot \mathsf{T}_n^{\epsilon} + \epsilon \nabla_{\boldsymbol{x}} \cdot \mathsf{T}_n^{\epsilon} = 0 \text{ in } \Omega_n, \tag{51}$$

$$\begin{aligned}\mathsf{T}_n^{\epsilon} &= -p_n^{\epsilon}\mathsf{I} + \epsilon\left(\nabla_{\boldsymbol{y}}\boldsymbol{v}_n^{\epsilon} + (\nabla_{\boldsymbol{y}}\boldsymbol{v}_n^{\epsilon})^{\mathsf{T}}\right) \\ &+ \epsilon^2\left(\nabla_{\boldsymbol{x}}\boldsymbol{v}_n^{\epsilon} + (\nabla_{\boldsymbol{x}}\boldsymbol{v}_n^{\epsilon})^{\mathsf{T}}\right),\end{aligned} \tag{52}$$

$$\nabla_{\boldsymbol{y}} \cdot \boldsymbol{v}_n^{\epsilon} + \epsilon \nabla_{\boldsymbol{x}} \cdot \boldsymbol{v}_n^{\epsilon} = 0, \text{ in } \Omega_n, \tag{53}$$

$$\mathsf{T}_n^{\epsilon}\boldsymbol{n} = \mathsf{T}_p^{\epsilon}\boldsymbol{n} \text{ on } \Gamma, \tag{54}$$

$$(\boldsymbol{v}_n^{\epsilon} - \dot{\boldsymbol{u}}^{\epsilon}) \cdot \boldsymbol{n} = \left((\tilde{\alpha} - 1)\dot{\boldsymbol{u}}^{\epsilon} + \boldsymbol{w}_p^{\epsilon}\right) \cdot \boldsymbol{n} \text{ on } \Gamma, \tag{55}$$

$$\boldsymbol{\tau}_{\beta} \cdot (\mathsf{T}_n^{\epsilon}\boldsymbol{n}) = -\epsilon\frac{\alpha}{\sqrt{\bar{k}}}(\boldsymbol{v}_n^{\epsilon} - \dot{\boldsymbol{u}}^{\epsilon}) \cdot \boldsymbol{\tau}_{\beta}, \text{ on } \Gamma, \tag{56}$$

$$\epsilon\boldsymbol{n} \cdot (\mathsf{T}_n^{\epsilon}\boldsymbol{n}) + \frac{1}{\bar{L}_p}(\boldsymbol{v}_n^{\epsilon} - \dot{\boldsymbol{u}}^{\epsilon}) \cdot \boldsymbol{n} = -\epsilon p_p^{\epsilon} \text{ on } \Gamma, \tag{57}$$

where the fields $\boldsymbol{w}_p^{\epsilon}$, $\boldsymbol{v}_n^{\epsilon}$, p_p^{ϵ}, p_n^{ϵ}, $\boldsymbol{u}^{\epsilon}$, T_p^{ϵ}, T_n^{ϵ} are the power series counterparts (cf. equation (46)) of $\boldsymbol{w}_p$, $\boldsymbol{v}_n$, p_p, p_n, $\boldsymbol{u}$, T_p, T_n, respectively. Since $\boldsymbol{y}$-periodicity is assumed, it is sufficient to consider the above conditions on the periodic cell (which we also call Ω). We further identify Ω_p and Ω_n with their corresponding periodic cell's portion.

In the following section, we equate the same power of ϵ in the relationships (47-57) for $\epsilon^{(l)} = l = 0, 1....$ We obtain a number of conditions that is used to determine (a) a new system of PDEs that describe the behavior of vascularized poroelastic materials on the macroscale $\boldsymbol{x}$ in terms of the leading (zero-th) order fields, (b) a new constitutive relationship that characterize the macroscale mechanical response of such a material, and (c) microscale cell problems which are to be solved to determine the coefficients of the resulting homogenized model.

5 Derivation of the homogenized model

The aim of this section is the derivation of a closed system of PDEs for the leading order variables $\boldsymbol{w}_p^{(0)}$, $\boldsymbol{v}_n^{(0)}$,

$p_p^{(0)}$, $p_n^{(0)}$, $\boldsymbol{u}^{(0)}$ over the macroscale domain spanned by the variable $\boldsymbol{x}$. This is done exploiting the conditions that arise equating the same power of $\epsilon^{(0)}$ and ϵ^1 in (47–57).

Since we aim at obtaining a system of PDEs that holds on the macroscale only, it is useful to define the following cell average operator

$$\langle(\bullet)\rangle_\kappa = \frac{1}{|\Omega|}\int_{\Omega_\kappa}(\bullet)\,\mathrm{d}\boldsymbol{y} \quad \kappa = p, n, \tag{58}$$

where $|\Omega|$ and $|\Omega_k|$ are the volumes of the periodic cell and its κ-portion. The specific cell average operator is defined as

$$\overline{\langle(\bullet)\rangle}_k = \frac{1}{|\Omega_\kappa|}\int_{\Omega_\kappa}(\bullet)\,\mathrm{d}\boldsymbol{y} \quad \kappa = p, n, \tag{59}$$

and the two operators are related by

$$\langle(\bullet)\rangle_\kappa = \phi_\kappa\overline{\langle(\bullet)\rangle}_\kappa, \tag{60}$$

where

$$\phi_\kappa = \frac{|\Omega_\kappa|}{|\Omega|} \quad \kappa = p, n, \tag{61}$$

is the volume fraction of the poroelastic (fluid network) compartment.

Remark 4 Note that the medium is not, in general, *macroscopically uniform*, i.e. the periodic cell can also exhibit variations with respect to the macroscale $\boldsymbol{x}$ (see e.g. [13, 20, 34, 35] and [12, 15]). However, investigation of such variations is not the primary aim here, therefore, we simply assume that $\Omega_\kappa = \Omega_\kappa(\boldsymbol{y})$, such that

$$\nabla_{\boldsymbol{x}}\cdot\int_{\Omega_\kappa}(\bullet)\,\mathrm{d}\boldsymbol{y} = \int_{\Omega_\kappa}\nabla_{\boldsymbol{x}}\cdot(\bullet)\,\mathrm{d}\boldsymbol{y}, \tag{62}$$

and the volume fractions ϕ_κ defined by (61) are constants. □

We equate the same powers of ϵ^0 in the system (47-57) to obtain:

$$\nabla_{\boldsymbol{y}}\cdot\mathsf{T}_p^{(0)} = 0 \text{ in } \Omega_p, \tag{63}$$
$$\mathbb{C}:\nabla_{\boldsymbol{y}}\boldsymbol{u}^{(0)} = 0 \text{ in } \Omega_p, \tag{64}$$
$$\nabla_{\boldsymbol{y}}p_p^{(0)} = 0 \text{ in } \Omega_p, \tag{65}$$
$$\tilde{\alpha}\bar{M}\nabla_{\boldsymbol{y}}\cdot\dot{\boldsymbol{u}}^{(0)} + \bar{M}\nabla_{\boldsymbol{y}}\cdot\boldsymbol{w}_p^{(0)} = 0 \text{ in } \Omega_p, \tag{66}$$
$$\nabla_{\boldsymbol{y}}\cdot\mathsf{T}_n^{(0)} = 0 \text{ in } \Omega_n, \tag{67}$$
$$\mathsf{T}_n^{(0)} = -p^{(0)}\mathsf{I}, \tag{68}$$
$$\nabla_{\boldsymbol{y}}\cdot\boldsymbol{v}_n^{(0)} = 0 \text{ in } \Omega_n, \tag{69}$$
$$\mathsf{T}_n^{(0)}\boldsymbol{n} = \mathsf{T}_p^{(0)}\boldsymbol{n} \text{ on } \Gamma, \tag{70}$$
$$(\boldsymbol{v}_n^{(0)} - \dot{\boldsymbol{u}}^{(0)})\cdot\boldsymbol{n} = \left((\tilde{\alpha}-1)\dot{\boldsymbol{u}}^{(0)} + \boldsymbol{w}_p^{(0)}\right)\cdot\boldsymbol{n} \text{ on } \Gamma, \tag{71}$$
$$\boldsymbol{\tau}_\beta\cdot(\mathsf{T}_n^{(0)}\boldsymbol{n}) = 0 \text{ on } \Gamma, \tag{72}$$
$$(\boldsymbol{v}_n^{(0)} - \dot{\boldsymbol{u}}^{(0)})\cdot\boldsymbol{n} = 0 \text{ on } \Gamma, \tag{73}$$

while the conditions obtained equating the same powers of ϵ^1 read:

$$\nabla_{\boldsymbol{y}}\cdot\mathsf{T}_p^{(1)} + \nabla_{\boldsymbol{x}}\cdot\mathsf{T}_p^{(0)} = 0 \text{ in } \Omega_p, \tag{74}$$
$$\mathsf{T}_p^{(0)} = \mathbb{C}:\nabla_{\boldsymbol{y}}\boldsymbol{u}^{(1)} + \mathbb{C}:\nabla_{\boldsymbol{x}}\boldsymbol{u}^{(0)} - \tilde{\alpha}p_p^{(0)}\mathsf{I}, \text{ in } \Omega_p, \tag{75}$$
$$\boldsymbol{w}_p^{(0)} = -\bar{k}\nabla_{\boldsymbol{y}}p_p^{(1)} - \bar{k}\nabla_{\boldsymbol{x}}p_p^{(0)}, \text{ in } \Omega_p, \tag{76}$$
$$\dot{p}_p^{(0)} = -\tilde{\alpha}\bar{M}\nabla_{\boldsymbol{y}}\cdot\dot{\boldsymbol{u}}^{(1)} - \bar{M}\nabla_{\boldsymbol{y}}\cdot\boldsymbol{w}_p^{(1)} - \tilde{\alpha}\bar{M}\nabla_{\boldsymbol{x}}\cdot\dot{\boldsymbol{u}}^{(0)} - \bar{M}\nabla_{\boldsymbol{x}}\cdot\boldsymbol{w}_p^{(0)}\text{ , in } \Omega_p, \tag{77}$$
$$\nabla_{\boldsymbol{y}}\cdot\mathsf{T}_n^{(1)} + \nabla_{\boldsymbol{x}}\cdot\mathsf{T}_n^{(0)} = 0 \text{ in } \Omega_n, \tag{78}$$
$$\mathsf{T}_n^{(1)} = -p_n^{(1)}\mathsf{I} + \left(\nabla_{\boldsymbol{y}}\boldsymbol{v}_n^{(0)} + (\nabla_{\boldsymbol{y}}\boldsymbol{v}_n^{(0)})^{\mathsf{T}}\right) \tag{79}$$
$$\nabla_{\boldsymbol{y}}\cdot\boldsymbol{v}_n^{(1)} + \nabla_{\boldsymbol{x}}\cdot\boldsymbol{v}_n^{(0)} = 0, \text{ in } \Omega_n, \tag{80}$$
$$\mathsf{T}_n^{(1)}\boldsymbol{n} = \mathsf{T}_p^{(1)}\boldsymbol{n} \text{ on } \Gamma, \tag{81}$$
$$(\boldsymbol{v}_n^{(1)} - \dot{\boldsymbol{u}}^{(1)})\cdot\boldsymbol{n} = \left((\tilde{\alpha}-1)\dot{\boldsymbol{u}}^{(1)} + \boldsymbol{w}_p^{(1)}\right)\cdot\boldsymbol{n} \text{ on } \Gamma, \tag{82}$$
$$\boldsymbol{\tau}_\beta\cdot(\mathsf{T}_n^{(1)}\boldsymbol{n}) = -\frac{\alpha}{\sqrt{\bar{k}}}(\boldsymbol{v}_n^{(0)} - \dot{\boldsymbol{u}}^{(0)})\cdot\boldsymbol{\tau}_\beta \text{ on } \Gamma, \tag{83}$$
$$\boldsymbol{n}\cdot\left(\mathsf{T}_n^{(0)}\boldsymbol{n}\right) + \frac{1}{\bar{L}_p}\left(\boldsymbol{v}_n^{(1)} - \dot{\boldsymbol{u}}^{(1)}\right)\cdot\boldsymbol{n} = -p_p^{(0)} \text{ on } \Gamma, \tag{84}$$

where we notice that, by means of condition (68), relationship (72) is actually just an identity. Equations (65) and (67-68) imply that $p_p^{(0)}$ and $p_n^{(0)}$ are $\boldsymbol{y}$-constant, respectively, i.e.

$$p_p^{(0)} = p_p^{(0)}(\boldsymbol{x}, t), \tag{85}$$
$$p_n^{(0)} = p_n^{(0)}(\boldsymbol{x}, t). \tag{86}$$

Equation (64) implies that $\nabla_{\boldsymbol{y}}\boldsymbol{u}^{(0)}$ is skew-symmetric, i.e, $\boldsymbol{u}^{(0)}$ is a rigid body motion. The only periodic solution of this type is $\boldsymbol{y}$-constant, that is

$$\boldsymbol{u}^{(0)} = \boldsymbol{u}^{(0)}(\boldsymbol{x}, t). \tag{87}$$

Enforcing condition (87) relationship (66) for the poroelastic compartment reduces to

$$\nabla_{\boldsymbol{y}}\cdot\boldsymbol{w}_p^{(0)} = 0 \text{ in } \Omega_p. \tag{88}$$

We now derive the effective governing equations for the vascularized poroelastic material systematically. We first describe the macroscale fluid dynamics in both the poroelastic and the fluid network compartments. We relate the cell average (cf. operator (58)) of the zeroth order velocities $\boldsymbol{w}_p^{(0)}$ and $\boldsymbol{v}_n^{(0)}$, respectively, to the leading order pressures $p_p^{(0)}$, $p_n^{(0)}$, and the macroscale displacement of the solid part $\boldsymbol{u}^{(0)}$. We then derive the homogenized stress balance equation and constitutive relationship for the material in terms of the leading order pressures and elastic displacement. Finally, we close the system of macroscale PDEs via two scalar equations for $p_p^{(0)}$ and $p_n^{(0)}$, highlighting the role of mass exchange between the two compartments.

5.1 Interstitial flow

We start substituting relationship (76) into the local divergence free constraint (88) to obtain a Laplace problem for $p_p^{(1)}(\boldsymbol{x}, \boldsymbol{y}, t)$

$$\nabla_{\boldsymbol{y}}^2 p_p^{(1)} = 0 \text{ in } \Omega_p. \tag{89}$$

The problem (89) is supplemented by $\boldsymbol{y}$-periodic conditions on $\partial\Omega_p/\Gamma$ and the non-homogeneous Neumann interface condition

$$\nabla_{\boldsymbol{y}} p_p^{(1)} \cdot \boldsymbol{n} = -\left(\nabla_{\boldsymbol{x}} p_p^{(0)} + (\tilde{\alpha}-1)\dot{\boldsymbol{u}}^{(0)}\right) \cdot \boldsymbol{n} \text{ on } \Gamma. \tag{90}$$

The above condition is obtained accounting for relationship (73), and then substituting (76) into the equation dictating continuity of the leading order normal component of relative velocities (71). The compatibility condition for the Laplace problem (89) reads

$$\int_\Gamma \left(\nabla_{\boldsymbol{x}} p_p^{(0)} + (\tilde{\alpha}-1)\dot{\boldsymbol{u}}^{(0)}\right) \cdot \boldsymbol{n} \, \mathrm{dS}_y = 0, \tag{91}$$

and it is fulfilled as the vector valued function

$$\boldsymbol{f}_m := \nabla_{\boldsymbol{x}} p_p^{(0)} + (\tilde{\alpha}-1)\dot{\boldsymbol{u}}^{(0)} \tag{92}$$

does not depend on the microscale variable $\boldsymbol{y}$ by means of relationships (87) and (85), so that

$$\int_\Gamma \boldsymbol{f}_m \cdot \boldsymbol{n} \, \mathrm{dS}_y = \int_{\partial\Omega_p} \boldsymbol{f}_m \cdot \boldsymbol{n} \, \mathrm{dS}_y = \\ - \int_{\Omega_p} \nabla_{\boldsymbol{y}} \cdot \boldsymbol{f}_m \, \mathrm{d}\boldsymbol{y} = 0, \tag{93}$$

where we have used $\boldsymbol{y}$-periodicity to transform the interface integral into a surface integral, have applied the divergence theorem with respect to $\boldsymbol{y}$, and exploited the fact that $\boldsymbol{f}_m$ is $\boldsymbol{y}$-constant.

Since the problem (89-90) is linear and (85), (87) hold, the following solution ansatz

$$p_p^{(1)} = -\boldsymbol{P}_p(\boldsymbol{y}) \cdot (\nabla_{\boldsymbol{x}} p_p^{(0)}(\boldsymbol{x}, t) + (1-\tilde{\alpha})\dot{\boldsymbol{u}}^{(0)}(\boldsymbol{x}, t)), \tag{94}$$

is its actual (up to a $\boldsymbol{y}$-constant function) solution, provided that the auxiliary vector $\boldsymbol{P}_p$ solves the following cell problem:

$$\nabla_{\boldsymbol{y}}^2 \boldsymbol{P}_p = 0 \qquad \text{in } \Omega_t \tag{95}$$

$$(\nabla_{\boldsymbol{y}} \boldsymbol{P}_p)\boldsymbol{n} = \boldsymbol{n} \qquad \text{on } \Gamma. \tag{96}$$

The problem (95-96) is equipped with $\boldsymbol{y}$-periodic condititions on $\partial\Omega_p/\Gamma$ and is to be closed by an additional constraint in order to ensure uniqueness, for example

$$\langle \boldsymbol{P}_p \rangle_p = \boldsymbol{0}. \tag{97}$$

We substitute ansatz (94) into relationship (76) and apply the average operator (58) to obtain the macroscale governing equations for the global average leading order relative velocity in the poroelastic compartment, i.e.

$$\left\langle \boldsymbol{w}_p^{(0)} \right\rangle_p = -\bar{k}\mathsf{G}\nabla_{\boldsymbol{x}} p_p^{(0)} + \bar{k}(\tilde{\alpha}-1)\langle \mathsf{P} \rangle_p \, \dot{\boldsymbol{u}}^{(0)}, \tag{98}$$

where the second rank tensor G reads

$$\mathsf{G} = \phi_p \mathsf{I} - \langle \mathsf{P} \rangle_p \tag{99}$$

or, componentwise

$$G_{ij} = \phi_p \delta_{ij} - \langle P_{ij} \rangle_p \tag{100}$$

and we defined

$$\mathsf{P} = \left\langle (\nabla_y \boldsymbol{P}_p)^{\mathsf{T}} \right\rangle_p, \tag{101}$$

that is, by components

$$P_{ij} = \left\langle \frac{\partial P_p^j}{\partial y_i} \right\rangle_p, \tag{102}$$

$i, j = 1, 2, 3$. In terms of the specific average (cf. (59)) equation (98) reads

$$\overline{\left\langle \boldsymbol{w}_p^{(0)} \right\rangle_p} = -\bar{k}\tilde{\mathsf{G}}_p \nabla_{\boldsymbol{x}} p_p^{(0)} + \bar{k}(\tilde{\alpha}-1)\overline{\langle \mathsf{P} \rangle}_p \dot{\boldsymbol{u}}^{(0)}, \tag{103}$$

where

$$\tilde{\mathsf{G}} = \mathsf{I} - \overline{\langle \mathsf{P} \rangle}_p. \tag{104}$$

According to equation (98), the poroelastic interstitial flow is driven by both the macroscopic pressure gradient and the leading order elastic velocity. The (non-dimensional) second rank tensor $\bar{k}\mathsf{G}$ given by the relationship (99) reads as an effective hydraulic conductivity for the poroelastic compartment. The leading order relative interstitial velocity is further corrected by an anisotropic contribution that is proportional to $(\tilde{\alpha}-1)$, i.e. it reduces to zero when the comprising solid matrix is incompressible.

5.2 Network flow

We start substituting the leading and first order fluid network stress tensor components (68) and (79), respectively, into the balance equation (78), such that, accounting for the leading order incompressibility constraint (69), we obtain the following relationship for $(\boldsymbol{v}_n^{(0)}, p_n^{(1)})$

$$\nabla_{\boldsymbol{y}}^2 \boldsymbol{v}_n - \nabla_{\boldsymbol{y}} p_n^{(1)} - \nabla_{\boldsymbol{x}} p_n^{(0)} = 0 \text{ in } \Omega_n. \tag{105}$$

The above equation, together with the incompressibility constraint (69) and interface conditions (83) and (71), can be rewritten as a Stokes' problem for $(\boldsymbol{w}_n^{(0)}, p_n^{(1)})$,

where $\boldsymbol{w}_n^{(0)}$ is the relative fluid network leading order velocity defined by

$$\boldsymbol{w}_n^{(0)} := \boldsymbol{v}_n^{(0)} - \dot{\boldsymbol{u}}^{(0)}. \tag{106}$$

Thus we have

$$\nabla_{\boldsymbol{y}}^2 \boldsymbol{w}_n^{(0)} - \nabla_{\boldsymbol{y}} p_n^{(1)} - \nabla_{\boldsymbol{x}} p_n^{(0)} = 0, \text{ in } \Omega_n \tag{107}$$

$$\nabla_{\boldsymbol{y}} \cdot \boldsymbol{w}_n^{(0)} = 0, \text{ in } \Omega_n \tag{108}$$

$$\boldsymbol{\tau}_\beta \cdot \left(\left(\nabla_{\boldsymbol{y}} \boldsymbol{w}_n^{(0)} + (\nabla_{\boldsymbol{y}} \boldsymbol{w}_n^{(0)})^{\mathsf{T}} \right) \boldsymbol{n} \right) = -\frac{\alpha}{\sqrt{\bar{k}}} \boldsymbol{w}_n^{(0)} \cdot \boldsymbol{\tau}_\beta, \text{ on } \Gamma \tag{109}$$

$$\boldsymbol{w}_n^{(0)} \cdot \boldsymbol{n} = 0, \text{ on } \Gamma, \tag{110}$$

where we have enforced that $\boldsymbol{u}^{(0)}$ is $\boldsymbol{y}$-constant (cf. equation (87). The solution of the PDEs system (107-110) can be deduced exploiting linearity and considering that the leading order pressure $p_n^{(0)}$ is $\boldsymbol{y}$-constant (cf. equation (86)). In fact, we have

$$\boldsymbol{w}_n^{(0)}(\boldsymbol{x}, \boldsymbol{y}, t) = -\mathsf{W}(\boldsymbol{y}) \nabla_{\boldsymbol{x}} p_n^{(0)}(\boldsymbol{x}, t) \tag{111}$$

$$p_n^{(1)}(\boldsymbol{x}, \boldsymbol{y}) = -\boldsymbol{P}_n(\boldsymbol{y}) \cdot \nabla_{\boldsymbol{x}} p_n^{(0)}(\boldsymbol{x}, t), \tag{112}$$

and the ansatz (111-112) is the solution of the problem provided that the auxiliary variables $(\mathsf{W}, \boldsymbol{P}_n)$ solve the following Stokes'-type cell problem:

$$\nabla_{\boldsymbol{y}} \boldsymbol{P}_{\boldsymbol{n}} = \nabla_{\boldsymbol{y}}^2 \mathsf{W}^{\mathsf{T}} + \mathsf{I} \text{ in } \Omega_n \tag{113}$$

$$\nabla_{\boldsymbol{y}} \cdot \mathsf{W}^{\mathsf{T}} = 0 \quad \text{in } \Omega_n \tag{114}$$

$$\mathsf{W}^{\mathsf{T}} \boldsymbol{n} = 0 \quad \text{on } \Gamma \tag{115}$$

$$[\left(\nabla_{\boldsymbol{y}} \mathsf{W}^{\mathsf{T}} + (\nabla_{\boldsymbol{y}} \mathsf{W}^{\mathsf{T}})^{\mathsf{T}} \right) \boldsymbol{n}] \boldsymbol{\tau}_\beta = \mathsf{W}^{\mathsf{T}} \boldsymbol{\tau}_\beta \text{ on } \Gamma. \tag{116}$$

The system (113-116) is equipped with $\boldsymbol{y}$-periodic conditions on $\partial\Omega_n/\Gamma$. In order to guarantee uniqueness for the auxiliary vector $\boldsymbol{P}_n$, we need a further vector condition, for example

$$\langle \boldsymbol{P}_n \rangle_n = 0. \tag{117}$$

The macroscale flow in the fluid network, which is described by relative fluid network average velocity, is obtained averaging (111)

$$\left\langle \boldsymbol{w}_n^{(0)} \right\rangle_n = -\mathsf{K} \nabla_{\boldsymbol{x}} p_n^{(0)}, \tag{118}$$

where K is the fluid network hydraulic conductivity tensor defined by

$$\mathsf{K} = \langle W \rangle_n \tag{119}$$

or, by components

$$K_{ij} = \langle W_{ij} \rangle \quad i, j = 1, 2, 3. \tag{120}$$

In terms of the specific average (cf. (59)) equation (118) reads

$$\overline{\left\langle \boldsymbol{w}_n^{(0)} \right\rangle}_n = \tilde{\mathsf{K}} \nabla_{\boldsymbol{x}} p_n^{(0)}, \tag{121}$$

where

$$\tilde{\mathsf{K}} = \overline{\langle W \rangle}_n. \tag{122}$$

The relative macroscale flow in the network is governed by an anisotropic Darcy's law and it is driven by the zero-th order fluid network pressure $p_n^{(0)}$, with (non-dimensional) hydraulic conductivity K given by (119).

5.3 Effective poromechanics

We now aim to determine the effective stress balance equation and constitutive relationship for vascularized poroelastic materials. Since the leading order poroelastic stress tensor also depends on the first order displacement $\boldsymbol{u}^{(1)}$, we first recover the latter as a function of leading order fields only. We start from the zero-th order stress balance equation substituting (75) into (63). We then obtain a linear elastic-type problem for the variable $\boldsymbol{u}^{(1)}$. We then enforce that $\boldsymbol{u}^{(0)}$, $p_p^{(0)}$ (cf. (85), (87)) are $\boldsymbol{y}$-constant and substitute the leading order characterization of the poroelastic and fluid network stress tensors (75) and (68), respectively, into interface conditions (70) to obtain the following linear elastic-type boundary value cell problem equipped with non-homogeneous Neumann interface conditions

$$\nabla_{\boldsymbol{y}} \cdot \left(\mathbb{C} : \nabla_{\boldsymbol{y}} \boldsymbol{u}^{(1)} \right) = 0 \tag{123}$$

$$(\mathbb{C} : \nabla_{\boldsymbol{y}} \boldsymbol{u}^{(1)}) \boldsymbol{n} = -(\mathbb{C} : \nabla_{\boldsymbol{x}} \boldsymbol{u}^{(0)}) \boldsymbol{n} + \tilde{\alpha} p_p^{(0)} \boldsymbol{n} - p_n^{(0)} \boldsymbol{n} \text{ on } \Gamma, \tag{124}$$

supplemented by $\boldsymbol{y}$-periodic conditions on $\partial\Omega_p/\Gamma$. The right hand side of equation (123) reduces to zero as $\boldsymbol{u}^{(0)}$, $p_p^{(0)}$, and the coefficients (in particular $\mathbb{C}$) are $\boldsymbol{y}$-constant.

Here, $\boldsymbol{u}^{(1)}$ is $\boldsymbol{y}$-periodic and the solution is unique up to an arbitrary $\boldsymbol{y}$-constant vector field. We exploit linearity of the problem (123-124), together with (85), (86), and (87) to formulate the following ansatz

$$\boldsymbol{u}^{(1)}(\boldsymbol{x}, \boldsymbol{y}, t) = \mathcal{A}(\boldsymbol{y}) \nabla_{\boldsymbol{x}} \boldsymbol{u}^{(0)}(\boldsymbol{x}, t) + \boldsymbol{a}(\boldsymbol{y}) \left(p_n^{(0)}(\boldsymbol{x}, t) - \tilde{\alpha} p_p^{(0)}(\boldsymbol{x}, t) \right) \tag{125}$$

in terms of the auxiliary third rank tensor and vector $\mathcal{A}$ (represented componentwise as A_{ijk}, $i, j, k = 1, 2, 3$) and $\boldsymbol{a}$, respectively.

The above ansatz solves the problem (123-124), provided that $\mathcal{A}$ and $\boldsymbol{a}$ are the solutions of the following periodic cell problems

$$\nabla_{\boldsymbol{y}} \cdot (\mathbb{C} : \nabla_{\boldsymbol{y}} \boldsymbol{a}) = \boldsymbol{0} \text{ in } \Omega_p \tag{126}$$

$$(\mathbb{C} : \nabla_{\boldsymbol{y}} \boldsymbol{a})\, \boldsymbol{n} = -\boldsymbol{n} \text{ on } \Gamma, \tag{127}$$

$$\frac{\partial}{\partial y_j}\left(C_{ijkl}\frac{\partial A_{k\nu\gamma}}{\partial y_l}\right) = 0 \text{ in } \Omega_p \tag{128}$$

$$C_{ijkl}\frac{\partial A_{k\nu\gamma}}{\partial y_l} n_j + C_{ij\nu\gamma} n_j = 0, \text{ on } \Gamma, \tag{129}$$

where $i, j, k, l, \nu, \gamma = 1...3$ and Einstein convention for summation over repeated indices is understood. The cell problems for the third rank tensor A_{ijk} and vectors $\boldsymbol{a}$, $\boldsymbol{b}$ are to be closed by a further condition, e.g.

$$\langle \boldsymbol{a} \rangle_p = 0, \ \langle A_{ijk} \rangle_p = 0 \ \forall \ i, j, k = 1...3. \tag{130}$$

The leading order poroelastic stress tensor, substituting (125) into (75), reads

$$\mathsf{T}_p^{(0)} = (\mathbb{C}\mathbb{M} + \mathbb{C}) : \nabla_{\boldsymbol{x}} u^{(0)} + (\mathbb{C} : \mathsf{Q}) p_n^{(0)} - \tilde{\alpha}\,(\mathbb{C} : \mathsf{Q} + \mathsf{I})\, p_p^{(0)}, \tag{131}$$

where the fourth rank tensor $\mathbb{M}$ and the second rank tensor Q are defined as

$$\mathbb{M} = \nabla_{\boldsymbol{y}} \mathcal{A}, \ \mathsf{Q} = \nabla_{\boldsymbol{y}} \boldsymbol{a}, \tag{132}$$

where $\mathbb{M}$ reads, by components

$$M_{kl\nu\gamma} = \frac{\partial A_{k\nu\gamma}}{\partial y_l}, \quad k, \nu, \gamma, l = 1, 2, 3. \tag{133}$$

Note that $\mathbb{M}$ is equipped with both minor symmetries, as it can be verified enforcing the corresponding minor symmetries of the tensor $\mathbb{C}$ in (128-129), and that the periodic cell problems, as written in the compact form (128-129) correspond to six elastic-type periodic cell problems, for each fixed (ν, γ), $\nu \geq \gamma, \quad \nu, \gamma = 1, 2, 3$.

Remark 5 Since we are assuming that the coefficients, and in particular $\mathbb{C}$, are just constants, they are in particular $\boldsymbol{y}$-constant and the solution for $\boldsymbol{u}^{(1)}$ can be equivalently written as

$$\boldsymbol{u}^{(1)}(\boldsymbol{x}, \boldsymbol{y}, t) = \tilde{\mathcal{A}}(\boldsymbol{y})(\mathbb{C} : \nabla_{\boldsymbol{x}} \boldsymbol{u}^{(0)})(\boldsymbol{x}, t) + \boldsymbol{a}(\boldsymbol{y}) \left(p_n^{(0)}(\boldsymbol{x}, t) - \tilde{\alpha} p_p^{(0)}(\boldsymbol{x}, t)_p\right), \tag{134}$$

where the third rank tensor $\tilde{\mathcal{A}}$ solves the following cell problem (up to a further condition, as for $\mathcal{A}$)

$$\frac{\partial}{\partial y_j}\left(C_{ijkl}\frac{\partial \tilde{A}_{k\nu\gamma}}{\partial y_l}\right) = 0 \text{ in } \Omega_p \tag{135}$$

$$C_{ijkl}\frac{\partial \tilde{A}_{k\nu\gamma}}{\partial y_l} n_j + \delta_{i\nu}\delta_{j\gamma} n_j = 0, \text{ on } \Gamma, \tag{136}$$

where $i, j, k, l, \nu, \gamma = 1...3$, Einstein convention for summation over repeated indices is understood. Defining

$$\mathbb{L} = \nabla_{\boldsymbol{y}} \tilde{\mathcal{A}} \tag{137}$$

and comparing the $\boldsymbol{y}$-gradient of the equivalent ansatzes (125) and (134) we obtain

$$\mathbb{M} = \mathbb{L}\mathbb{C}. \tag{138}$$

We further note, although the presence of both pressure fields plays a role in determining the solution for $\boldsymbol{u}^{(1)}$, the functional form of the cell problems (126-127) and (128-129) is the same as the standard poroelastic setting (up to the volume force contributions proportional to the derivatives of $\mathbb{C}$ that do not appear here as we are in the homogeneous setting), see [13, 27]. In particular, the following relationship holds:

$$\langle \mathrm{tr}\mathbb{M} \rangle_p = \langle \mathbb{C} : \mathbb{Q} \rangle_p \,, \tag{139}$$

that is, by components

$$\langle M_{kkij} \rangle_p = \langle C_{ijlm} Q_{lm} \rangle_p \,. \tag{140}$$

Relationship (139) can be deduced exploiting the properties of the cell problems (126-127) and (128-129), and applying (several times) the divergence theorem with respect to the local variable $\boldsymbol{y}$, exactly as done in the appendix of [13], where the due steps are (equivalently) carried out assuming local boundedness instead of periodicity.[4] □

We now proceed in determining the homogenized stress balance and constitutive equation for the vascularized poroelastic material. We perform global average (58) of the first order stress balance equations (74) and (78) on the corresponding cell portions Ω_p and Ω_n, obtaining the following macroscale equations

$$-\frac{1}{|\Omega|}\int_\Gamma \mathsf{T}_p^{(1)} \boldsymbol{n} \, \mathrm{dS}_y + \nabla_{\boldsymbol{x}} \cdot \left\langle \mathsf{T}_p^{(0)} \right\rangle_p = 0, \tag{141}$$

$$\frac{1}{|\Omega|}\int_\Gamma \mathsf{T}_n^{(1)} \boldsymbol{n} \, \mathrm{dS}_y + \nabla_{\boldsymbol{x}} \cdot \left\langle \mathsf{T}_n^{(0)} \right\rangle_n = 0, \tag{142}$$

where, in both cases, we have applied the divergence theorem in $\boldsymbol{y}$ and $\boldsymbol{y}$-periodicity to cancel the surface contributions on $\partial\Omega_p$ and $\partial\Omega_n$. Furthermore, we have applied, in both cases, macroscopic uniformity (62). We now sum up equations (141) and (142) and account for order one continuity of stresses (81) to finally obtain

[4] Note that in the appendix reported in [13] the third rank tensor v_p^{ij} is equivalent to our $\mathcal{A}$ and its gradient to our $\mathbb{M}$. However, the latter is always identified to $\mathbb{L}\mathbb{C}$, although relationship (138) actually rigorously holds only when $\mathbb{C}$ is locally constant.

the homogenized stress balance equation for the vascularized poroelastic material

$$\nabla_{\boldsymbol{x}} \cdot \mathsf{T}_{vp} = 0, \tag{143}$$

where $\mathsf{T}_{vp} = \left\langle \mathsf{T}_n^{(0)} \right\rangle_n + \left\langle \mathsf{T}_p^{(0)} \right\rangle_p$. Accounting for the leading order relationships for the fluid network and poroelastic stress tensors (68) and (131), yields

$$\mathsf{T}_{vp} = \langle (\mathbb{C}\mathbb{M} + \mathbb{C}) \rangle_p : \nabla_{\boldsymbol{x}} u^{(0)} + \left(\langle \mathbb{C} : \mathsf{Q} \rangle_p - \phi_n \mathsf{I} \right) p_n^{(0)} - \tilde{\alpha} (\langle \mathbb{C} : \mathsf{Q} \rangle_p + \phi_p \mathsf{I}) p_p^{(0)}. \tag{144}$$

The new constitutive equation for the material (144) dictates the mechanical response of the whole medium on the macroscale. The effective stress tensor T_{vp} encodes both an elastic-type contribution (proportional to the leading order displacement gradient) and role of the interstitial and network pressures.

We have now derived Darcy's macroscale equations for the interstitial flow (98) and the network flow (118), as well the stress balance equations for the medium (143-144). Therefore, we have specified nine equations for the behavior of the leading order relative interstitial velocity $\boldsymbol{w}_p^{(0)}$, network velocity $\boldsymbol{w}_n^{(0)}$, and elastic displacement $\boldsymbol{u}^{(0)}$. To close the system of macroscale PDEs we derive two scalar differential equations that determine the pressures $p_p^{(0)}$ and $p_n^{(0)}$ and account for the contribution due to fluid transport between the poroelastic and fluid network compartments.

5.4 Effective governing equations for vascularized poroelastic materials

We start averaging the order one fluid network constraint (80) to obtain

$$\nabla_{\boldsymbol{x}} \cdot \left\langle \boldsymbol{v}_n^{(0)} \right\rangle_n = -\frac{1}{|\Omega|} \int_{\Gamma} \boldsymbol{v}_n^{(1)} \cdot \boldsymbol{n} \, \mathrm{dS}_y, \tag{145}$$

where we have applied macroscopic uniformity (62) on the left hand side of (145) and the divergence theorem (together with periodicity to cancel out surface contribution on $\partial\Omega_n$) with respect to $\boldsymbol{y}$ on the right hand side. Substituting relationship (84) into (145) yields

$$\nabla_{\boldsymbol{x}} \cdot \left\langle \boldsymbol{v}_n^{(0)} \right\rangle_n = -\frac{|\Gamma| \bar{L}_p}{|\Omega|} (p_n^{(0)} - p_p^{(0)}) - \frac{1}{|\Omega|} \int_{\Gamma} \dot{\boldsymbol{u}}^{(1)} \cdot \boldsymbol{n} \, \mathrm{dS}_y, \tag{146}$$

where we have considered (85-86), and $|\Gamma|$ is the total surface of the interface Γ. We now apply back the divergence theorem (and $\boldsymbol{y}$-periodicity) with respect to $\boldsymbol{y}$ on the right hand side of (146), obtaining

$$-\frac{1}{|\Omega|} \int_{\Gamma} \dot{\boldsymbol{u}}^{(1)} \cdot \boldsymbol{n} \, \mathrm{dS}_y = \frac{1}{|\Omega|} \int_{\Omega_p} \nabla_{\boldsymbol{y}} \cdot \dot{\boldsymbol{u}}^{(1)} \, \mathrm{d}\boldsymbol{y}, \tag{147}$$

where we have considered that $\boldsymbol{n}$ is pointing out of the fluid network region. We substitute the solution (125) for $\boldsymbol{u}^{(1)}$ and exploit the auxiliary tensors definitions (132) to obtain

$$\nabla_{\boldsymbol{x}} \cdot \left\langle \boldsymbol{v}_n^{(0)} \right\rangle_n = -\frac{|\Gamma| \bar{L}_p}{|\Omega|} (p_n^{(0)} - p_p^{(0)}) + \hat{f}(\boldsymbol{x}, t), \tag{148}$$

where we have defined

$$\hat{f} = \langle \mathrm{tr}\mathbb{M} \rangle_p : \nabla_{\boldsymbol{x}} \dot{\boldsymbol{u}}^{(0)} + \langle \mathrm{tr}\mathsf{Q} \rangle_p \, \dot{p}_n^{(0)} - \tilde{\alpha} \, \langle \mathrm{tr}\mathsf{Q} \rangle_p \, \dot{p}_p^{(0)}, \tag{149}$$

enforcing the identity $\nabla_{\boldsymbol{y}} \cdot \dot{\boldsymbol{u}}^{(1)} = \mathrm{tr}(\nabla_{\boldsymbol{y}} \dot{\boldsymbol{u}}^{(1)})$. The scalar constraint in terms of pressures and elastic displacement only is obtained exploiting Darcy's relationship (118) and (106) and reads

$$\nabla_{\boldsymbol{x}} \cdot (\mathsf{K} \nabla_{\boldsymbol{x}} p_n^{(0)}) - \phi_n \nabla_{\boldsymbol{x}} \cdot \dot{\boldsymbol{u}}^{(0)} = \frac{|\Gamma| \bar{L}_p}{|\Omega|} (p_n^{(0)} - p_p^{(0)}) - \hat{f}. \tag{150}$$

We are now left with the last equation to close the final system of macroscale PDEs. Averaging the constraint (77) over Ω_p yields

$$\nabla_{\boldsymbol{x}} \cdot \left\langle \boldsymbol{w}_p^{(0)} \right\rangle_p = -\phi_p \frac{\dot{p}_p^{(0)}}{\bar{M}} - \tilde{\alpha} \hat{f} + \frac{1}{|\Omega|} \int_{\Gamma} \boldsymbol{w}_p^{(1)} \cdot \boldsymbol{n} - \phi_p \tilde{\alpha} \nabla_{\boldsymbol{x}} \cdot \dot{\boldsymbol{u}}^{(0)}, \tag{151}$$

where we have applied again macroscopic uniformity on the left hand side of (151), and the divergence theorem in $\boldsymbol{y}$ (together with $\boldsymbol{y}$-periodicity) to obtain the interface integral involving $\boldsymbol{w}_p^{(1)}$. Finally, we exploit the interface condition (82) together with mass exchange dictated by (84), and exploit the corrected Darcy relationship (98) to formulate the last scalar differential equation as follows

$$\nabla_{\boldsymbol{x}} \cdot (\bar{k} \mathsf{G} \nabla_{\boldsymbol{x}} p_p^{(0)}) = \bar{k}(\tilde{\alpha} - 1) \, \langle \mathsf{P} \rangle_p \, \nabla_{\boldsymbol{x}} \cdot \dot{\boldsymbol{u}}^{(0)} + \phi_p \frac{\dot{p}_p^{(0)}}{\bar{M}} + \hat{f} + \frac{|\Gamma| \bar{L}_p}{|\Omega|} (p_p^{(0)} - p_n^{(0)}) + \phi_p \tilde{\alpha} \nabla_{\boldsymbol{x}} \cdot \dot{\boldsymbol{u}}^{(0)}. \tag{152}$$

Equations (152) and (150) close the systems of effective governing equations for the vascularized poroelastic material.

In the next section, we perform a thorough discussion concerning the new model we have derived and we illustrate key particular cases which may be of interest for practical applications.

6 Discussion and interpretation of the results

In Section 5 we have derived the new system of PDEs that describes the macroscopic behavior of vascularized poroelastic materials. It consists of the two scalar equations (150), (152) and the three vector-valued equations (equivalent to nine scalar equations) (98), (118), and (143) in terms of the leading order pressure fields $p_n^{(0)}(\boldsymbol{x},t)$, $p_p^{(0)}(\boldsymbol{x},t)$, relative velocities $\left\langle \boldsymbol{w}_n^{(0)} \right\rangle_n(\boldsymbol{x},t)$, $\left\langle \boldsymbol{w}_p^{(0)} \right\rangle_p(\boldsymbol{x},t)$, and elastic displacement $\boldsymbol{u}^{(0)}(\boldsymbol{x},t)$.

These PDEs can be rearranged, for every $\boldsymbol{x} \in \Omega_H$ and for every $t \in (0,T)$, $T \in \mathbb{R}^+$, as follows

$$
\begin{cases}
\nabla_{\boldsymbol{x}} \cdot \mathsf{T}_{vp} = 0 & (153)\\
\dfrac{\dot{p}_n^{(0)}}{M_{vp}} = -\nabla_{\boldsymbol{x}} \cdot \left\langle \boldsymbol{w}_n^{(0)} \right\rangle_n - (\phi_n \mathsf{I} - \langle \mathbb{C} : \mathsf{Q} \rangle_p) : \nabla_{\boldsymbol{x}} \dot{\boldsymbol{u}}^{(0)} & (154)\\
\quad + \dfrac{\tilde{\alpha}}{M_{vp}} \dot{p}_p^{(0)} - \dfrac{|\Gamma| \bar{L}_p}{|\Omega|}(p_n^{(0)} - p_p^{(0)})\\
\dot{p}_p^{(0)} \left(\dfrac{\phi_p}{\bar{M}} + \dfrac{\tilde{\alpha}}{M_{vp}} \right) = -\nabla_{\boldsymbol{x}} \cdot \left\langle \boldsymbol{w}_p^{(0)} \right\rangle_p + \dfrac{\dot{p}_n^{(0)}}{M_{vp}} & (155)\\
\quad - (\tilde{\alpha}\phi_p \mathsf{I} + \langle \mathbb{C} : \mathsf{Q} \rangle_p) : \nabla_{\boldsymbol{x}} \dot{\boldsymbol{u}}^{(0)} - \dfrac{|\Gamma| \bar{L}_p}{|\Omega|}(p_p^{(0)} - p_n^{(0)})\\
\left\langle \boldsymbol{w}_n^{(0)} \right\rangle_n = -\mathsf{K} \nabla_{\boldsymbol{x}} p_n^{(0)} & (156)\\
\left\langle \boldsymbol{w}_p^{(0)} \right\rangle_p = -\bar{k} \mathsf{G} \nabla_{\boldsymbol{x}} p_p^{(0)} + \bar{k}(\tilde{\alpha} - 1) \langle \mathsf{P} \rangle_p \dot{\boldsymbol{u}}^{(0)}, & (157)
\end{cases}
$$

where we recall that the global constitutive relationship is given by (144), i.e.

$$
\mathsf{T}_{vp} = \langle (\mathbb{C}\mathbb{L}\mathbb{C} + \mathbb{C}) \rangle_p : \nabla_{\boldsymbol{x}} u^{(0)} + \left(\langle \mathbb{C} : \mathsf{Q} \rangle_p - \phi_n \mathsf{I} \right) p_n^{(0)}
$$
$$
- \tilde{\alpha}(\langle \mathbb{C} : \mathsf{Q} \rangle_p + \phi_p \mathsf{I}) p_p^{(0)},
$$

where we set

$$
M_{vp} = -\frac{1}{\langle \mathrm{tr} \mathsf{Q} \rangle_p}. \tag{158}
$$

Equations (153-157) constitute a closed macroscale system of PDEs.

Remark 6 (Cell problems and computational feasibility) The model is capable to account for a large variety of physical phenomena at a reduced computational cost. In fact, given the input, homogeneous parameters and a suitable prescription of the geometry of the periodic cell Ω, the coefficient are as well homogeneous, and are to be computed solving periodic cell problems which solely depend on the microscale local variable $\boldsymbol{y}$. In particular, the hydraulic conductivity K (cf. equation (119)) and second rank tensor $\langle \mathsf{P} \rangle_p$ (which is in turn required to compute the interstitial conductivity G, cf. equation (99)) involve the solution of the cell problems (113-116) and (95-96), respectively. The Stokes'-type cell problem in the compact tensorial form (113-116) is analogous to that derived for rigid structures in [34, 41] and actually corresponds, in general, to three Stokes' problems, as noted in [35]. In the latter work, the authors solve the model [41] in three dimensions and provide an example of numerical solution of these cell problems for a prototypical tortuous geometry representative of the tumor microvasculature. They also solve the cell problems on the interstitial complementary geometry, which formally coincide with the problems (95-96). These correspond, in general, to three standard Laplace's problems. The fourth and second rank auxiliary tensors $\mathbb{L}$ and Q (cf. relationships (132) and (137)) are to be computed solving the elastic-type cell problem (126-127) and the six elastic-type cell problems given corresponding to (135-136), or equivalently (128-129), as in our case (138) holds. The systems of PDEs (128-129) and (126-127) actually correspond to those arising in standard poroelasticity [13, 27], specialized for homogeneous coefficients. An example of a suitable computational approach for the solution of three dimensional periodic, elastic-type cell problems for composite materials (which possess a similar structure, but are more complex as they involve discontinuity of the elastic constants across the interface between phases) is given in [36], and applied to the bone hierarchical structure in [37]. Once the coefficients are computed solving the cell problems only once and independently of the macroscale, then it suffices to insert the Darcy-type relationships (156-157) into their corresponding scalar relationships (154-155), and the constitutive relationship (144) into (153) to obtain a coupled system of five scalar differential equations for the five unknowns $p_p^{(0)}$, $p_n^{(0)}$, and the three components of $\boldsymbol{u}$. The solution can be finally computed on the macroscale domain Ω_H where microscale variations are smoothed out, provided that appropriate initial conditions and boundary conditions on $\partial\Omega_H$ are prescribed, and the velocities recovered back via (156-157). □

The system of effective governing equations for a vascularized poroelastic material (153-157) formally reads as an anisotropic *double poroelastic model* equipped with source terms. It globally accounts for the mutual interplay of (a) fluid flow in the network, (b) interstitial flow in the pores, (c) strains of the comprising elastic matrix, (d) fluid transport between the poroelastic and fluid network compartment. We discuss the physical meaning of the various terms and parameters arising in the next sections below.

6.1 Effective elasticity tensor for the vascularized poroelastic material

The effective constitutive relationship (144) accounts for the mechanical response of the whole material. It comprises both a linear elastic contribution, and the mechanical response due to the pores and network pressures. The relative importance of the latter is also dictated by the microstructure geometry, which is encoded in the second rank tensor $\langle \mathbb{C} : \mathsf{Q} \rangle_p$. The effective elasticity tensor for a vascularized poroelastic material is given by

$$\mathbb{C}_{vp} = \langle (\mathbb{C}\mathbb{L}\mathbb{C} + \mathbb{C}) \rangle_p \,, \tag{159}$$

where $\mathbb{C}$ is the elasticity tensor of the poroelastic phase and $\mathbb{L}$ is given by (137). The latter is to be computed solving microscale cell problems that depend on both the elastic properties of the poroelastic phase and on the microscale geometry. The effective elastic tensor for a poroelastic material is in general anisotropic also for an isotropic poroelastic elasticity tensor (see (7)) and it retains the same functional form as the poroelastic elasticity tensor that is obtained applying asymptotic homogenization to a standard fluid-structure interaction problem between a Newtonian fluid and a linear elastic solid in a porous structure [13]. However, the cell problems which are indeed formally analogous to those of standard poroelasticity) are to be computed on the microscale, where only geometric variations of the network are relevant, as the pore scale variations are already smoothed out by means of the poroelasticity assumption, and the dependency on the latter is encoded in the poroelastic elasticity tensor $\mathbb{C}$.

6.2 A double Darcy model for the relative velocities

The macroscale fluid network and interstitial velocities (relative to the actual and corrected solid velocities) are described by Darcy's laws (156-157), with non-dimensional hydraulic conductivities given by K and $\bar{k}\mathsf{G}$, respectively. In particular, the relationship for the relative interstitial velocity (157) is equipped with a correction term which depends on the microstructure and vanishes whenever both the fluid phase and the solid phase in the poroelastic compartment are intrinsically incompressible, i.e. for $\tilde{\alpha} = 1$. In the latter case, (157) just reads as a standard Darcy's law for the inetrstitial velocity, further averaged over the whole domain. Relationship (156) is the Darcy law for the average velocity in the network, relative to solid velocity, and it formally appears as the standard Darcy's relative velocity profile that would be experienced by fluid velocity in a porous, linear elastic material, although the solid velocity is affected by the both the network and the interstitial flow in this case.

6.3 Effective coefficients of the double poroelastic model

The two scalar equations (155-154) that close the global system of PDEs physically represent the balance of interstitial and fluid network volumes variations, which are affected by the strains of the (potentially compressible) elastic matrix and by the fluid transport between the two compartments as a consequence of fluid extravasation from the vessels/channels network. The structure of these relationships is analogous to that of a mass balance constraint (with sources) in poroelasticity, as it comprises, in both cases, pressure variations in time, variations of fluid and solid volumes, and source terms which provide the coupling between the two. Hence, the model can be formally regarded as *double poroelastic*. However, the physical meaning of the coefficient multiplying a particular contribution in the governing equation of one fluid phase does not necessarily coincide with its corresponding counterpart in the governing equation of the other fluid phase. Furthermore, the coupling source term for one fluid phase is both related to the fluid transport between compartments (proportional to the pressure jump, as in the double porosity fluid transport models [34, 41]) and to the influence of pressure's time variations in the other fluid phase. These features, which arise mathematically as a natural consequence of the upscaling process, uniquely characterize this particular model, which is therefore different from standard phenomenological double poroelastic models which can be found in the literature (see, e.g. [2] as an example of double poroelastic model for the coupling of fluid flow through deformable fractures and elastic matrix. In this case, the only source term is proportional to the fluid pressure difference and the physical interpretation of parameters is that of a single poroelastic model for each fluid phase). However, the arising parameters (and terms) have a clear physical interpretation, as we discuss below.

The coefficient M_{vp} (cf. (158)) is the opposite of the inverse of $\langle \mathrm{tr}\mathsf{Q} \rangle_p$, where the latter is given by (132) and is to be comptuted solving the elastic type cell problem (126-127). The latter cell problem, as well as the functional form of M_{vp} as a function of the auxiliary tensor Q, are analogous to that found in standard poroelasticity for the characterization of the Biot modulus in terms of the pore structure (when the fluid flowing in the pores is incompressible). However, its dependencies and physical meaning do not coincide with

those of the standard Biot's modulus, although a connection can be found. In fact, even though the Biot modulus can be in principle computed solving a cell problem formally identical to (126-127)[13], the latter is to be solved on the pore scale geometry and enforcing the *elastic* properties of the matrix. The coefficient M_{vp} defined here encodes, instead, geometric information on the microstructure (which is dictated by the interaction between the poroelastic medium and the fluid network vessels/channels), and the *poroelastic* elasticity tensor $\mathbb{C}$. In analogy with the standard Biot's modulus, M_{vp} can be interpreted as the variation of fluid network volume in response to an increase of the difference between the network and pore pressures, as though the elastic phase were intrinsically incompressible ($\tilde{\alpha} = 1$, $M \to +\infty$), at constant strains and up to the fluid extravasation between compartments (cf. (154)). The coefficient M_{vp} can be equivalently defined through equation (155) as the negative variation of the interstitial fluid volume under the same conditions described above and for the same increase of pressure difference (cf. (154), reflecting the balance of total fluid volume that is expected in such a case. It is worth remarking that the coefficient $1/M_{vp} = -\langle \mathrm{tr}\mathsf{Q} \rangle_p$ multiplying the time derivatives of the pressures in (154-155) is different from zero also for incompressiblity of the solid phase, as opposed to its classical Biot's counterpart. This is due to the fact that the second rank tensor Q depends on the elasticity tensor of the *poroelastic* material, which is filled by the fluid in the pores, and is not globally incompressible also when the elastic matrix and the interstitial fluid individually are (cf. constraint (14)). However, whenever solid deformations can be neglected, $\mathsf{Q} = \mathsf{0}$ (cf. equation (168)), and in turn $1/M_{vp} = -\langle \mathrm{tr}\mathsf{Q} \rangle_p = 0$. Therefore, our model automatically accounts for the mutual influence of time pressures' variations due to structure's deformations.

The second rank tensor $\phi_n \mathsf{I} - \langle \mathbb{C} : \mathsf{Q} \rangle_p$ that appears in (154) has the same functional form as its standard poroelastic counterpart (see, e.g. [13] and relationship (15)). In order to highlight its physical meaning, we specialize the term $(\phi_n \mathsf{I} - \langle \mathbb{C} : \mathsf{Q} \rangle_p) : \nabla_{\boldsymbol{x}} \dot{\boldsymbol{u}}$ that appear in (154) in the case of macroscale isotropy, obtaining

$$(\phi_n \mathsf{I} - \langle \mathbb{C} : \mathsf{Q} \rangle_p) : \nabla_{\boldsymbol{x}} \dot{\boldsymbol{u}} = \alpha_v \nabla_{\boldsymbol{x}} \dot{\boldsymbol{u}}^{(0)}, \tag{160}$$

where

$$\alpha_v = \phi_n - \frac{1}{3} \mathrm{tr} \langle \mathbb{C} : \mathsf{Q} \rangle_p . \tag{161}$$

The coefficient α_v is an effective Biot's coefficient relating fluid network volume and solid variations, as it represents the ratio of network fluid volume variations to solid volume variations for constant pressures and up to fluid extravasation. Its anisotropic counterpart is represented by the second rank tensor $\phi_n \mathsf{I} - \langle \mathbb{C} : \mathsf{Q} \rangle_p$. As for the coefficient M_v, α_v is in general different from one also when assuming that the solid phase is intrinsically incompressible, as opposed to its classical counterpart, as $(\mathbb{C} : \mathsf{Q})$, and in particular Q, is to be computed by means of $\mathbb{C}$ (cf. cell problem (126-127)), which represents the elastic stiffness of the poroelastic material.

The form of equations (155-154) ensures that a poroelastic mass balance of the type (10) is reached with respect to the macroscopic relative fluid velocity averaged over the whole domain (i.e. the sum of the average of the interstitial and fluid network velocities. The latter reads as the exact counterpart of relationship (14) whenever incompressibility of the solid phase is assumed, as in this case, the solid and fluid phases are intrinsically incompressible. We comment and justify these statements below.

6.4 Global mass conservation for the vascularized poroelastic material

We now show that a global mass conservation relationship of poroelastic-type holds for the vascularized poroelastic material. We sum equations (155) and (154) obtaining

$$\frac{\phi_p}{\bar{M}} \dot{p}_p^{(0)} = -\nabla_{\boldsymbol{x}} \cdot \boldsymbol{w}_{vp} - (\tilde{\alpha}\phi_p + \phi_n) \nabla_{\boldsymbol{x}} \cdot \dot{\boldsymbol{u}}^{(0)}, \tag{162}$$

where we defined the global fluid velocity in the vascularized poroelastic material as

$$\boldsymbol{w}_{vp} = \left\langle \boldsymbol{w}_p^{(0)} \right\rangle_p + \left\langle \boldsymbol{w}_n^{(0)} \right\rangle_n , \tag{163}$$

which has the same form as its analogous for a standard poroelastic material (cf. (10)) in terms of the global fluid velocity (163). Whenever the elastic phase is intrinsically incompressible, we then obtain the mass conservation constraint for the vascularized poroelastic material as a perfect balance of interstitial fluid, network fluid, and solid variations of volumes, as follows

$$\phi_n \nabla_{\boldsymbol{x}} \cdot \overline{\left\langle \boldsymbol{v}_n^{(0)} \right\rangle_n} + \phi\phi_p \nabla_{\boldsymbol{x}} \cdot \overline{\left\langle \boldsymbol{v}_p^{(0)} \right\rangle_p} + (1 - \phi_n - \phi\phi_p) \nabla_{\boldsymbol{x}} \cdot \dot{\boldsymbol{u}}^{(0)} = 0, \tag{164}$$

where we have enforced incompressibility of the solid matrix ($\tilde{\alpha} = 1$ and $\bar{M} \to +\infty$), and have exploited back the definitions of the network and interstitial relative fluid velocities (106) and (9), respectively, together with the specific average operators (59) and porosity definitions (61). The constraint (164) represents the global

mass conservation constraint when the three phases interacting in the medium are intrinsically incompressible. The volume fraction $\phi\phi_p$ represents the ratio between the volume of interstitial fluid flowing in the pores and the volume of the whole vascularized poroelastic material.

6.5 Comparison with the double porosity model derived in [34, 41]

We now show that the double porosity model derived in [41] and recovered as a particular case (for macroscopically uniform structures and purely Newtonian blood flow) in [34] coincides with our system of PDEs given by (154-157), for $p_p^{(0)}$, $p_n^{(0)}$, $\left\langle \boldsymbol{w}_p^{(0)} \right\rangle_p$, $\left\langle \boldsymbol{w}_n^{(0)} \right\rangle_n$, when the solid matrix comprising the porous compartment is rigid. In this case, for every $l = 0, 1, ...$, $\boldsymbol{u}^{(l)} = \boldsymbol{0}$. In particular,

$$\boldsymbol{u}^{(0)} = \boldsymbol{0}, \tag{165}$$

that implies

$$\boldsymbol{w}_p^{(0)} = \phi \boldsymbol{v}_p^{(0)}, \tag{166}$$

and

$$\boldsymbol{w}_n^{(0)} = \boldsymbol{v}_n^{(0)} \tag{167}$$

according to definitions (9) and (106), respectively. Since also $\boldsymbol{u}^{(1)} = \boldsymbol{0}$, we obtain

$$\mathsf{Q} = \mathsf{0}, \tag{168}$$

see (125), which also implies

$$\mathbb{C} : \mathsf{Q} = 0. \tag{169}$$

Applying conditions (165-169) to equations (154-157) we obtain, accounting for the specific averages (cf. definitions (59)):

$$\begin{cases} -\nabla_{\boldsymbol{x}} \cdot \overline{\left\langle \boldsymbol{v}_n^{(0)} \right\rangle_n} = \dfrac{|\Gamma|\bar{L}_p}{|\Omega_n|}(p_n^{(0)} - p_p^{(0)}) & (170) \\ -\nabla_{\boldsymbol{x}} \cdot \overline{\left\langle \phi \boldsymbol{v}_p^{(0)} \right\rangle_p} = \dfrac{|\Gamma|\bar{L}_p}{|\Omega_p|}(p_p^{(0)} - p_n^{(0)}) & (171) \\ \overline{\left\langle \boldsymbol{v}_n^{(0)} \right\rangle_n} = -\tilde{\mathsf{K}} \nabla_{\boldsymbol{x}} p_n^{(0)} & (172) \\ \overline{\left\langle \phi \boldsymbol{v}_p^{(0)} \right\rangle_p} = -\tilde{\mathsf{G}} \nabla_{\boldsymbol{x}} p_p^{(0)}. & (173) \end{cases}$$

The model in terms of pressures $p_p^{(0)}$, $p_n^{(0)}$ only reads, substituting (172-173) into (170-171):

$$\begin{cases} \nabla_{\boldsymbol{x}} \cdot \left(\tilde{\mathsf{K}} \nabla_{\boldsymbol{x}} p_n^{(0)} \right) = \dfrac{|\Gamma|\bar{L}_p}{|\Omega_n|}(p_n^{(0)} - p_p^{(0)}) & (174) \\ \nabla_{\boldsymbol{x}} \cdot \left(\tilde{\mathsf{G}} \nabla_{\boldsymbol{x}} p_p^{(0)} \right) = \dfrac{|\Gamma|\bar{L}_p}{|\Omega_p|}(p_p^{(0)} - p_n^{(0)}). & (175) \end{cases}$$

The double porosity model (174-175), with Darcy's velocities given by (172-173) and specific interstitial and network hydraulic conductivities defined by (104) and (122), respectively, exactly coincides, up to the notation[5] with the system of PDEs derived in [41] and obtained as a special case of [34] for the capillary and interstitial blood pressures and velocities in vascularized, rigid tumors.

Our model (153-157) for vascularized poroelastic materials therefore reads as the generalization of the double porosity model [41] to deformable solid structures.

Remark 7 (Vascularized tumors) In the context of tumor modeling, our new system of PDEs describes the macroscopic behavior of a vascularized deformable tumor mass with blood leakage from the vessels walls to the tumor mass. The model accounts for the dependency of both the pore (interstitial) and vascular pressures (as well as the corresponding velocities) on the complex interplay between tumor strains (potentially also for an intrinsically compressible elastic phase), blood extravasation, and microstructural properties of the blood vessels' network. The role and relative importance of the latter phenomena on the time-dependent pressures and velocities profiles can help in elucidating implications on drug delivery, providing novel hints for the designed of improved anti-cancer therapies based on informed injection conditions, thus extending the analysis carried out in [30]. In the latter work, the implications of tumor strains on the vascular pressure drop (which is assumed to drive drug delivery) is analyzed via a standard biphasic (i.e. the solid and interstitial fluid phase in the pores are assumed intrinsically incompressible) model for the porous compartment, whereas the microvasculature merely plays the role of a source term for the interstitial compartment. The role of the microstructural properties of the network, as well as that of spatio-temporal variations of the vascular pressure (which is assumed to be constant), are neglected. □

[5] See Section 4.3.1, pages 24-25, [34], and the model (4.100-4.103) therein, which is in turn proved to be equivalent to eqs. (54), (56), (70), (75) in [41]. In [34], the quantities $\tilde{\mathsf{K}}$, $\tilde{\mathsf{G}}$, p_p, $\boldsymbol{v}_n$, $\phi\boldsymbol{v}_p$, $|\Omega_p|$, $|\Gamma|$ are denoted by K, E, p_t, $\boldsymbol{u}_n$, $\boldsymbol{u}_t$, $|\Omega_t|$, S, respectively. Both in [41] and [34], only specific averages are used, and they are denoted as we denote non-specific averages, i.e. $\langle \bullet \rangle_k$.

In the next section, we conclude our manuscript summarizing the results and highlighting further perspectives.

7 Conclusions

We have presented a novel model that describes the behavior of *vascularized poroelastic materials*, i.e. deformable porous solids encoding a network of vessels or channels. These media represent real-world physical systems, such as vascularized tumors, hard biological tissues (e.g. bone and tendons), and fractured porous rocks. We have considered the (non-dimensional) fluid-structure interaction problem between an isotropic and homogeneous Biot's poroelastic compartment (30-33) and an incompressible Newtonian fluid network phase (34-36), in a quasi-static setting and in absence of body forces. The two compartments are coupled via the interface conditions (37-40), that arise from global conservation of momentum and fluid mass, slip of fluid over a porous surface and transport of fluid across the interface between the network and the porous interstitium. Next, we have enforced the length scale separation between the intervessels' distance (*microscale*) and the average medium size (*macroscale*) to apply the *asymptotic homogenization* technique and derive the new model (153-157). The results are systematically derived in section 5 and discussed in section 6.

The functional form of these equations is different from previously adopted, perfectly symmetric, double poroelastic phenomenological models (see, e.g., [2]), and it explicitly accounts for the mutual influence of the time variations of the pressures due to deformations of the porous matrix. Although the resulting anisotropic model can be formally regarded as *double-poroelastic*, it posesses specific peculiarities and coefficients that mathematically arise from the upscaling process, and physically account for the different influence of elastic deformations on the (pore) interstitial and network fluid phases, in a globally mass conserving setting.(cf. equations (162) and constraint (164) for intrinsically incompressible phases.)

The homogenized double poroelastic model (153-157) accounts for a large variety of physical phenomena at a reduced computational cost, as it is a linear system of PDEs to be solved on the macroscopic domain Ω_H, where microscale variations are smoothed out, see Figure 1. Nevertheless, information on the microstructure is encoded in the coefficients of the model, which are to be computed solving classical periodic cell problem solely on the microscale.

We have derived the model under a number of simplifying assumptions, although we have employed most of them to avoid complicating the notation and better highlight the physical significance of the model.

Our results can be readily generalized to linearized inertia and body forces in both the fluid network and the poroelastic compartment, as these contributions would appear in the stress balance equation (153) only as appropriate leading order time variations and body forces (similarly to [13]), but would neither modify the structure of the model's coefficients, nor the constitutive relationship (144) that dictates the mechanical response of the material. Following [13], compressibility of the fluid phases could be achieved introducing the fluid bulk modulus (thus admitting that Biot's modulus M also depends on the latter).

We have assumed that the poroelastic phase is homogeneous and that the fluid viscosity is constant. The poroelastic coefficients depend on the pore scale structure and geometry, as well as on the elasticity tensor of the solid comprising matrix; since these coefficients can be considered averaged on such a pore scale, they can exhibit inhomogeneities only if the latter are encoded in the elastic phase stiffness tensor and are relevant on the scale of the whole poroelastic compartment [13]. These variations can, in turn, be relevant both on the microscale and on the macroscale in our current formulation, as both these scales are much larger than the pore scale. Thus, our model can be generalized admitting that every parameter is inhomogeneous (as each of them retains a dependency on the solid elastic matrix).

Macroscale variations of the poroelastic coefficients would not formally affect any of the results presented here. The cell problems (126-127) and (128-129), and, in turn, the poroelastic coefficients, would retain a parametric dependence on the macroscale. As a consequence, the solution of the macroscale model would require the solution of these cell problem for each macroscale point, i.e., the computational cost would greatly increase. This argument also applies to the fluid network cell problem (113-116 when macroscale variations of the viscosity are permitted, as in [34]. This issue also arises when the structure is not macroscopically uniform (i.e. when macroscale variations of the microscale geometry are permitted) and suitable strategies are emerging in the literature to minimize the computational effort, see, e.g., [15].

Microscale variations of the coefficients would not result in an increase of the computational cost, although the structure of the cell problems would be affected by such changes. In particular, the standard volume force term accounting for microscale variations of the poroelastic stiffness tensor would appear on the right hand side of cell problem (128-129), whereas a new elastic-type cell problem would arise as a consequence of mi-

croscale variations of the Biot coefficient. Furthermore, variations of the latter would be required to satisfy the compatibility condition (91). We believe that the investigation of the effects of local inhomogeneities could be an interesting further development of the present model, at the time realistic variations of the elastic stiffness of the solid matrix are experimentally provided.

According to remark 2, the model can be readily generalized to anisotropic poroelastic compartments. Since experimental values of anisotropic poroelastic parameters are rarely provided in the literature, this extension would be particularly interesting whenever also the pore scale geometry is known. According to the latter scenario, the generalization of our main result (153-157) would read as a *three scale* model (macroscale, microscale, pore scale), as the effective coefficients would retain both the information on the microscale and on the pore scale explicitly, the latter being encoded in the input poroelastic parameters as shown in [13, 27]. An interesting alternative approach to account for the three scale explicitly relies on the so called reiterated homogenization, see, e.g. [28] as an example of application concerning poroelastic materials. In this case, it is not necessary to embrace effective mechanical models (such as poroelasticity) as a starting point, as two local variables are introduced to account explicitly for the length scale separation among the three scales involved in the problem. It would be an interesting task to derive an homogenized model for vascularized poroelastic materials via this approach (and compare results on cases of practical interest), and the challenge would reside in accounting for transport of fluid from the vessels walls, which can be more naturally handled starting from a fluid-structure interaction problem on the physical scale.

Our new model is further open to improvements in a number of areas. From a theoretical standpoint, the extension of such a model to growing poroelastic structure ([35]), as well transport of passive scalars, such as macromolecule drugs and nanoparticles (see, e.g., [34, 45, 46]) would represent challenging extensions to the model, that could be extremely relevant to several real-world physical systems, such as vascularized tumors.

Finally, the next natural step is to compare model predictions obtained via prescribed realistic geometries against experimental data related to an actual vascularized poroelastic material. This will not only enable model validation (via comparison against experimental data), but could highlight the interplay between the vessels' microstructure and the fluid transport in a deforming structure.

In the case of vascularized tumors, predictions from our model could elucidate the role of the microvascular structure on the spatio-temporal pressures' profile and suggest optimized injection conditions for anti-cancer therapies that rely on drug advection.

Acknowledgements

The authors are indebted to Davide Ambrosi, Alf Gerisch, and Rebecca Shipley for useful hints and discussions concerning the content of this manuscript.

Compliance with Ethical Standards

This study was funded by the Ministry of Economy in Spain, under the project reference DPI2014-58885-R. Conflict of Interest: The authors declare that they have no conflict of interest.

References

1. Auriault, J.L., Boutin, C., Geindreau, C.: Homogenization of coupled phenomena in heterogenous media, vol. 149. John Wiley & Sons (2010)
2. Bai, M., Meng, F., Elsworth, D., Abousleiman, Y., Roegiers, J.C.: Numerical modelling of coupled flow and deformation in fractured rock specimens. International journal for numerical and analytical methods in geomechanics **23**(2), 141–160 (1999)
3. Bakhvalov, N., Panasenko, G.: Homogenisation averaging processes in periodic media. Springer (1989)
4. Beavers, G.S., Joseph, D.D.: Boundary conditions at a naturally permeable wall. Journal of Fluid Mechanics **30**, 197–207 (1967)
5. Berryman, J.G.: Comparison of upscaling methods in poroelasticity and its generalizations. Journal of Engineering Mechanics **131**(9), 928–936 (2005)
6. Biot, M.: General solutions of the equations of elasticity and consolidation for a porous material. J. appl. Mech **23**(1), 91–96 (1956)
7. Biot, M.A.: General theory of three-dimensional consolidation. Journal of applied physics **12**(2), 155–164 (1941)
8. Biot, M.A.: Theory of elasticity and consolidation for a porous anisotropic solid. Journal of Applied Physics **26**(2), 182–185 (1955)
9. Biot, M.A.: Theory of propagation of elastic waves in a fluid-saturated porous solid. i. low-frequency range. The Journal of the acoustical Society of america **28**(2), 168–178 (1956)

10. Biot, M.A.: Mechanics of deformation and acoustic propagation in porous media. Journal of applied physics **33**(4), 1482–1498 (1962)
11. Bottaro, A., Ansaldi, T.: On the infusion of a therapeutic agent into a solid tumor modeled as a poroelastic medium. Journal of Biomechanical engineering **134**, 1–6 (2012)
12. Bruna, M., Chapman, S.J.: Diffusion in spatial varying porous media. SIAM Journal on Applied Mathematics **75**(4), 1648–1674 (2015)
13. Burridge, R., Keller, J.: Poroelasticity equations derived from microstructure. Journal of acoustical society of America **70**, 1140–1146 (1981)
14. Cowin, S.C.: Bone poroelasticity. Journal of biomechanics **32**(3), 217–238 (1999)
15. Dalwadi, M.P., Griffiths, I.M., Bruna, M.: Understanding how porosity gradients can make a better filter using homogenization theory. In: Proc. R. Soc. A, vol. 471, p. 20150464. The Royal Society (2015)
16. Detournay, E., Cheng, A.D.: Fundamentals of poroelasticity. In: C. Fairhurst (ed.) Comprehensive Rock Engineering: Principles, Practice and Projects, Vol. II, Analysis and Design Method, chap. 10, pp. 113–171. Pergamon Press, Oxford (2004)
17. Discacciati, M., Quarteroni, A.: Navier-stokes/darcy coupling: modeling, analysis, and numerical approximation. Revista Matemática Complutense **22**(2), 315–426 (2009)
18. Eshelby, J.: The determination of the elastic field of an ellipsoidal inclusion, and related problems. Proceedings of the Royal Society of London. Series A. Mathematical and Physical Sciences **241**, 376–396 (1957)
19. Gurtin, M., Fried, E., Anand, L.: The mechanics and thermodynamics of continua. Cambridge University press (2010)
20. Holmes, M.: Introduction to perturbation method. Springer-Verlag (1995)
21. Hornung, U.: Homogenization and porous media. Springer (1997)
22. Jain, R.K.: Transport of molecules across tumor vasculature. Cancer Metastasis Review **6**, 559–594 (1987)
23. Jain, R.K.: Physiological barriers to delivery of monoclonal antibodies and other macromolecules in tumors. Cancer Research **50**, 814–819 (1990)
24. Jain, R.K., Baxter, L.T.: Mechanisms of heterogeneous distribution of monoclonal antibodies and other macromolecules in tumors: significance of elevated interstitial pressure. Cancer Research **48**, 7022–7032 (1988)
25. Jones, I.P.: Low reynolds number flow past a porous spherical shell. Mathematical Proceedings of the Cambridge Phylosofical Society **73**, 231–238 (1973)
26. Kedem, O., Katchalsky, A.: Thermodynamic of the permeability of biological membranes to non-electrolytes. Biochimica and Biophysica Acta **27**, 229–246 (1958)
27. Mei, C.C., Vernescu, B.: Homogenization Methods for multiscale mechanics. World Scientific (2010)
28. Meirmanov, A.: Double porosity models for liquid filtration in incompressible poroelastic media. Mathematical Models and Methods in Applied Sciences **20**(04), 635–659 (2010)
29. Mikelić, A., Wheeler, M.F.: Convergence of iterative coupling for coupled flow and geomechanics. Computational Geosciences **17**(3), 455–461 (2013)
30. Netti, P.A., Baxter, L.T., Boucher, Y., Skalak, R., Jain, R.K.: Time-dependent behavior of interstitial fluid pressure in solid tumors: implications for drug delivery. Cancer Research **55**(22), 5451–5458 (1995)
31. Papanicolau, G., Bensoussan, A., Lions, J.L.: Asymptotic analysis for periodic structures. Elsevier (1978)
32. Coussy, O. Mechanics and physics of porous solids. John Wiley & Sons (2011).
33. Penta, R., Ambrosi, D.: The role of the microvascular tortuosity in tumor transport phenomena. Journal of theoretical biology **364**, 80–97 (2015)
34. Penta, R., Ambrosi, D., Quarteroni, A.: Multiscale homogenization for fluid and drug transport in vascularized malignant tissues. Mathematical Models and Methods in Applied Sciences **25**(1), 79–108 (2015)
35. Penta, R., Ambrosi, D., Shipley, R.J.: Effective governing equations for poroelastic growing media. The Quarterly Journal of Mechanics and Applied Mathematics **67**(1), 69–91 (2014)
36. Penta, R., Gerisch, A.: Investigation of the potential of asymptotic homogenization for elastic composites via a three-dimensional computational study. Computing and Visualization in Science **17**(4), 185–201 (2016)
37. Penta, R., Raum, K., Grimal, Q., Schrof, S., Gerisch, A.: Can a continuous mineral foam explain the stiffening of aged bone tissue? a micromechanical approach to mineral fusion in musculoskeletal tissues. Bioinspiration & biomimetics **11**(3), 035,004 (2016)
38. Saffman, P.G.: On the boundary condition at the surface of a porous medium. Studies in Applied Mathematics **50**(2), 93–101 (1971)

39. Sanchez-Palencia, E.: Non-Homogeneous Media and Vibration Theory-Lecture Notes in Physics 127. Springer-Verlag (1980)
40. Sanchez-Palencia, E.: Homogenization method for the study of composite media. Asymptotic analysis II-Lecture notes in mathematics **985**, 192–214 (1983)
41. Shipley, R.J., Chapman, J.: Multiscale modelling of fluid and drug transport in vascular tumors. Bulletin of Mathematical Biology. **72**, 1464–1491 (2010)
42. Showalter, R.E.: Poroelastic filtration coupled to stokes flow. Lecture Notes in Pure and Applied Mathematics **242**, 229–237 (2005)
43. Wang, H.: Theory of linear poroelasticity with applications to geomechanics and hydrogeology. Princeton University Press (2000)
44. Weiner, S., Wagner, H.D.: The material bone: Structure-mechanical function relations. Annual Reviews of Materials Science **28**, 271–298 (1998)
45. Mascheroni, P., Penta, R.: The role of the microvascular network structure on diffusion and consumption of anti-cancer drugs. Int J Numer Meth Biomed Engng. 2016; e2857. doi:10.1002/cnm.2857
46. Taffetani, M., de Falco, C., Penta, R., Ambrosi, D., Ciarletta, P.: Biomechanical modelling in nanomedicine: multiscale approaches and future challenges. Archive of Applied Mechanics. **84**(9-11), 1627–1645 (2014)